

# EPR paradox and quantum steering in a three-mode optomechanical system

Qiongyi He<sup>1,2\*</sup> and Zbigniew Ficek<sup>3</sup>

<sup>1</sup>*State Key Laboratory of Mesoscopic Physics, Department of Physics, Peking University, Beijing 100871, China*

<sup>2</sup>*Collaborative Innovation Center of Quantum Matter, Beijing 100871, China and*

<sup>3</sup>*The National Centre for Mathematics and Physics, KACST, P.O. Box 6086, Riyadh 11442, Saudi Arabia*

We study multi-partite entanglement, the generation of EPR states and quantum steering in a three-mode optomechanical system composed of an atomic ensemble located inside a single-mode cavity with a movable mirror. The cavity mode is driven by a short laser pulse, has a nonlinear parametric-type interaction with the mirror and a linear beamsplitter-type interaction with the atomic ensemble. There is no direct interaction of the mirror with the atomic ensemble. A threshold effect for the dynamics of the system is found, above which the system works as an amplifier and below which as an attenuator of the output fields. The threshold is determined by the ratio of the coupling strengths of the cavity mode to the mirror and to the atomic ensemble. It is shown that above the threshold the system effectively behaves as a two-mode system in which a perfect bipartite EPR state can be generated, while it is impossible below the threshold. Furthermore, a fully inseparable tripartite entanglement and even further a genuine tripartite entanglement can be produced above and below the threshold. In addition, we consider quantum steering and examine the monogamy relations that quantify the amount of bipartite steering that can be shared between different modes. It is found that the mirror is more capable for steering of entanglement than the cavity mode. The two way steering is found between the mirror and the atomic ensemble despite the fact that they are not directly coupled to each other, while it is impossible between the output of cavity mode and the ensemble which are directly coupled to each other.

## I. INTRODUCTION

The possibility of entangling macroscopic objects has been of interest for many years. Of particular interest is the possibility to entangle macroscopic objects using an optomechanical cavity containing a macroscopic mechanical oscillator such as a movable mirror or vibrating membrane [1–4]. In an optomechanical system the motion of the mechanical oscillator can be affected by the radiation pressure of the cavity field which may result in a parametric coupling between the cavity mode and the oscillator. The parametric couplings have long been known to produce nonclassical effects such as multimode squeezing and entanglement. Consequently, a number of papers have been devoted to the study of entanglement in optomechanical systems. Most of these studies considers two-mode optomechanical systems and explores entanglement in the steady-state [5–22]. Further studies have considered the generation of steady-state bipartite entanglement in three-mode systems [23–25].

In contrast to the numerous publications concerning the steady-state entanglement there are only a limited number of studies in transient (pulsed) regime. In terms of the difficulties in the creation of stationary entanglement, the pulsed regime could be free from the decoherence and dissipation effects such as the damping of the oscillating mirror. In addition, it could not be limited by the stability conditions imposed on the steady-state solutions. Pulsed excitation of a two-mode optomechanical

system has been treated by several authors in the context of the generation of EPR-type correlations between the pulse and a mechanical oscillator [26] and quantum steering [27]. When an optomechanical system is composed of more than two modes, more complex correlations can be created. These correlations can significantly affect the two-mode entanglement and result in multimode entanglement.

It is the purpose of this paper to study bipartite and tripartite entanglement in a three-mode system realized with an atomic ensemble located inside a single-mode cavity with a movable mirror. We work in the pulsed regime and concentrate on the ability of the system to generate perfect bipartite EPR states, fully inseparable and genuine tripartite entanglement and quantum steering. We assume that in the pulsed regime the relaxation effects of the mirror and the atoms can be neglected. In fact, it is not an overly restrictive limitation regarding a slow damping rate of the mirror and the existence of dipole transitions with relatively long relaxation times in some atoms [28]. We find a threshold effect for the dynamics of the system imposed by the ratio  $G/G_a$  of the coupling strengths of the oscillating mirror and the atoms to the cavity mode, respectively. Above the threshold ( $G > G_a$ ), the system behaves as an amplifier, whereas below the threshold ( $G < G_a$ ), the system behaves as an attenuator of the input laser pulses. The threshold behavior leads to substantially different results for the bipartite and tripartite entanglement above and below the threshold.

The paper is organized as follows. In Sec. II we develop a general formalism for the pulsed three-mode optomechanics. The formalism is based on solution the Heisen-

---

\*Electronic address: qiongyihe@pku.edu.cn

berg equations of motion, which is an extension of the work of Hofer *et al.* [26] to the case of three coupled modes. General expressions for the input-output relations between the quadrature components of the modes are derived and some of their properties are discussed along with a brief discussion of the variances of the quadrature components in the limit of large squeezing. Section III is concerned with bipartite entanglement between the modes. We adopt both the symmetric criterion of Duan, Giedke, Cirac, and Zoller (DGCZ) [29] and a less restrictive condition, based on asymmetric weightings of the quadratures [27, 30, 31] to examine the bipartite entanglement and the inseparability conditions as a function of the duration of the input laser pulse. Explicit analytic solutions are given for the parameters and the conditions for entanglement and the possibility to generate perfect EPR entangled states are determined. Section IV is devoted to tripartite entanglement. In searching for fully inseparable tripartite entanglement, we use the van Loock-Furusawa inequalities [32], and for the detection of genuine tripartite entanglement we use the criterion given by Shalm *et al.* [33] and Reid [34]. In Sec. V we concentrate on quantum steering and examine the monogamy relations that quantify the amount of bipartite steering that can be shared between different modes. We consider the monogamy relations and inequalities for quantum steering, recently proposed by Reid [35]. We summarize our results in Sec. VI. Finally, in the Appendix, we give the explicit expressions for the input-output relations between the quadrature components of the three modes of the system.

## II. PULSED THREE-MODE OPTOMECHANICS

We consider an optomechanical system composed of an ensemble of  $N$  identical two-level atoms located inside a single-mode cavity formed by two mirrors, a fixed semitransparent mirror and a movable fully reflective mirror, as shown in Fig. 1. The cavity mode is driven through the semitransparent mirror by a pulsed laser field, which is treated classically in our calculations and is characterized by its frequency  $\omega_L$  and a time dependent amplitude  $E(t)$ . We assume that the amplitude  $E(t)$  is constant over a short time interval  $0 \leq t \leq \tau$  and zero outside this interval. The cavity field is treated as quantized and is characterized by its frequency  $\omega_c$  and the annihilation and creation operators  $a_c$  and  $a_c^\dagger$ . The movable mirror is modeled as a quantized single-mode harmonic oscillator of frequency  $\omega_m$  and an amplitude determined by operators  $a_m$  and  $a_m^\dagger$ . The oscillations of the movable mirror result from the radiation pressure of the cavity field on the mirror. The atomic ensemble of identical two-level atoms, each composed of a ground state  $|g_j\rangle$  and an excited state  $|e_j\rangle$ , separated by the transition frequency  $\omega_a$ , interacts with the cavity mode and is represented by the collective dipole lowering, raising, and population difference operators,  $S^- = \sum_j |g_j\rangle\langle e_j|$ ,  $S^+ = \sum_j |e_j\rangle\langle g_j|$ , and

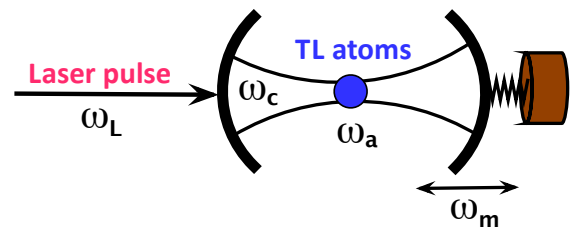


Figure 1: (Color online) Schematic diagram of the system. An ensemble of identical two-level (TL) atoms, each of transition frequency  $\omega_a$ , is located inside a single-mode cavity of frequency  $\omega_c$ . The cavity mode is driven by a laser pulse of frequency  $\omega_L$  and the movable mirror oscillates with frequency  $\omega_m$ .

$S_z = \sum_j (|e_j\rangle\langle e_j| - |g_j\rangle\langle g_j|)$ , respectively. We assume that the coupling of the atoms to the cavity mode is weak so that the excitation probability of the atomic ensemble is very small,  $S_z \approx \langle S_z \rangle \approx -N$ . In this case, we may represent the collective dipole lowering and raising operators in terms of bosonic annihilation and creation operators,  $c_a = S^- / \sqrt{|\langle S_z \rangle|}$  and  $c_a^\dagger = S^+ / \sqrt{|\langle S_z \rangle|}$ , respectively. It is easily verified that the operators  $c_a$  and  $c_a^\dagger$  satisfy the fundamental commutation relation for boson operators,  $[c_a, c_a^\dagger] = 1$ .

The total Hamiltonian  $H$  of the system, including the laser driving field and the nonlinear radiation pressure interaction between the cavity mode and the mirror, can be written as

$$H = H_c + H_a + H_m + H_I, \quad (1)$$

where

$$H_c = \hbar\omega_c a_c^\dagger a_c \quad (2)$$

is the free Hamiltonian of the cavity mode of frequency  $\omega_c$ ,

$$H_a = \hbar\omega_a c_a^\dagger c_a \quad (3)$$

is the free Hamiltonian of the atomic excitation mode of frequency  $\omega_a$ ,

$$H_m = \hbar\omega_m a_m^\dagger a_m \quad (4)$$

is the free Hamiltonian of the movable mirror oscillating with frequency  $\omega_m$ , and

$$H_I = \hbar g_a (c_a^\dagger a_c + a_c^\dagger c_a) + \hbar g_0 a_c^\dagger a_c (a_m^\dagger + a_m) + i\hbar [E(t)a_c^\dagger e^{-i\omega_L t} - E^*(t)a_c e^{i\omega_L t}] \quad (5)$$

is the interaction Hamiltonian of the cavity mode with the atomic mode, the external driving field, and with the movable mirror. Here,  $g_a$  is the coupling constant between the atoms and the cavity mode,  $g_0$  is the coupling constant between the cavity mode and the movable mirror, and  $E$  is the amplitude of the laser field. Note that

the atomic mode is not directly coupled to the mechanical mode and the interaction between the cavity and mechanical modes involves the nonlinear optomechanical coupling [23, 26].

To remove the terms oscillating with the laser frequency  $\omega_L$  in Eq. (5), we introduce the evolution operator

$$U(t) = e^{i\omega_L(a_c^\dagger a_c + c_a^\dagger c_a)t}, \quad (6)$$

which transforms the Hamiltonian (1) into

$$\begin{aligned} \tilde{H} &\equiv U(t) \left( H - i\hbar \frac{d}{dt} \right) U^\dagger(t) \\ &= \hbar\Delta_c a_c^\dagger a_c + \hbar\Delta_a c_a^\dagger c_a + \hbar\omega_m a_m^\dagger a_m \\ &\quad + \hbar g_a (c_a^\dagger a_c + a_c^\dagger c_a) + \hbar g_0 a_c^\dagger a_c (a_m^\dagger + a_m) \\ &\quad + i\hbar [E(t)a_c^\dagger - E^*(t)a_c], \end{aligned} \quad (7)$$

where  $\Delta_c = \omega_c - \omega_L$  and  $\Delta_a = \omega_a - \omega_L$  are the detunings of the atomic frequency  $\omega_c$  and the cavity mode frequency  $\omega_a$ , respectively, from the driving field frequency  $\omega_L$ . Note that in practice, the frequency  $\omega_m$  is much smaller than the laser, atomic and cavity frequencies and, therefore, can be comparable to the detunings  $\Delta_c$  and  $\Delta_a$ .

The Hamiltonian (7) involves the nonlinear optomechanical coupling between the cavity mode and the oscillating mirror, which results from the radiation pressure of the cavity field on the mirror. In the limit of a strong driving,  $|E_L| \gg g_0, g_a$ , the Hamiltonian (7) can be significantly simplified and the driving term eliminated by going into a displaced picture, in which each operator is written as the sum of its steady-state value and a small linear displacement

$$c_a \rightarrow \alpha_a + \delta c_a, \quad a_m \rightarrow \alpha_m + \delta a_m, \quad a_c \rightarrow \alpha_c + \delta a_c. \quad (8)$$

The displacement operators satisfy the Gaussian statistics and are delta correlated in time such that all the first moments vanish,

$$\langle \delta c_a \rangle = \langle \delta a_m \rangle = \langle \delta a_c \rangle = 0, \quad (9)$$

and for the second moments we suppose that the only nonzero are

$$\begin{aligned} \langle \delta c_a(t) \delta c_a^\dagger(t') \rangle &= \langle \delta a_c(t) \delta a_c^\dagger(t') \rangle = \delta(t-t'), \\ \langle \delta a_m(t) \delta a_m^\dagger(t') \rangle &= (n_0 + 1) \delta(t-t'), \\ \langle \delta a_m^\dagger(t) \delta a_m(t') \rangle &= n_0 \delta(t-t'), \end{aligned} \quad (10)$$

where  $n_0 = [\exp(\hbar\omega_m/k_B T) - 1]^{-1}$  is the mean number of the thermal photons at the frequency of the mechanical mode,  $k_B$  is the Boltzmann constant and  $T$  is the temperature of the environment surrounding the mirror. In other words, we assume that the cavity mode and the atom are in the ordinary zero temperature environment, whereas the mirror is in a thermal field of a nonzero temperature.

Taking only the quadratic terms of the displacement operators, we arrive to an effective Hamiltonian

$$\begin{aligned} H_{eff} &= \hbar\Delta_a \delta c_a^\dagger \delta c_a + \hbar\omega_m \delta a_m^\dagger \delta a_m + \hbar\Delta'_c \delta a_c^\dagger \delta a_c \\ &\quad + \hbar g_a (\delta c_a^\dagger \delta a_c + \delta a_c^\dagger \delta c_a) \\ &\quad + \hbar g (\delta a_c + \delta a_c^\dagger) (\delta a_m + \delta a_m^\dagger), \end{aligned} \quad (11)$$

where  $\Delta'_c = \Delta_c + g_0(\alpha_m + \alpha_m^*)$  and  $g = g_0|\alpha_c|$ .

The Hamiltonians (11) leads to the following Heisenberg equations of motion for the displacement operators

$$\begin{aligned} \delta \dot{a}_m &= -(\gamma_m + i\omega_m) \delta a_m - ig(\delta a_c + \delta a_c^\dagger) - \sqrt{2\gamma_m} \xi_{in}, \\ \delta \dot{a}_c &= -(\kappa + i\Delta'_c) \delta a_c - ig_a \delta c_a \\ &\quad - ig(\delta a_m^\dagger + \delta a_m) - \sqrt{2\kappa} a_{in}, \\ \delta \dot{c}_a &= -(\gamma_a + i\Delta_a) \delta c_a - ig_a \delta a_c - \sqrt{2\gamma_a} c_{in}, \end{aligned} \quad (12)$$

where we have included damping rates of the modes and the corresponding noise operators.

Our purpose of this paper is to examine entangled properties of the three modes and quantum steering. It is well known that these properties are strongly sensitive to losses. For this reason we shall work in the bad cavity limit of  $\kappa \gg g_a, g$  and consider a short evolution time of the system determined by the damping rate of the cavity mode,  $t \sim 1/\kappa$ . It has an advantage that over the short evolution time  $t \sim 1/\kappa$ , the relaxations of the atom and the mechanical mirror can be neglected ( $\gamma_a = \gamma_m = 0$ ) together with the corresponding noise terms,  $\xi_{in} = c_{in} = 0$ .

In order to solve Eq. (12), it is convenient to introduce slowly varying variables which are free from the oscillations at the frequency  $\omega_m$  and are related to the annihilation operators by

$$\begin{aligned} \delta a_m^r &= \delta a_m e^{i\omega_m t}, \quad \delta a_c^r = \delta a_c e^{-i\omega_m t}, \\ \delta c_a^r &= \delta c_a e^{-i\omega_m t}, \quad a_{in}^r = a_{in} e^{-i\omega_m t}. \end{aligned} \quad (13)$$

In terms of these new variables and after dropping the damping and noise terms of the atomic and mechanical modes, Eq. (12) becomes

$$\begin{aligned} \delta \dot{a}_m^r &= -ig \delta a_c^r e^{2i\omega_m t} - ig(\delta a_c^r)^\dagger, \\ \delta \dot{a}_c^r &= -[\kappa + i(\Delta'_c + \omega_m)] \delta a_c^r - ig_a \delta c_a^r \\ &\quad - ig(\delta a_m^r)^\dagger - ig \delta a_m^r e^{-2i\omega_m t} - \sqrt{2\kappa} a_{in}^r, \\ \delta \dot{c}_a^r &= -i(\Delta_a + \omega_m) \delta c_a^r - ig_a \delta a_c^r, \end{aligned} \quad (14)$$

in which we recognize certain terms oscillating at twice the frequency  $\omega_m$ . When the equations are integrated over times  $\omega_m t \gg 1$ , these oscillatory terms make a negligible contribution and therefore we may safely ignore them. After discarding the fast oscillating terms, which is a form of the rotating-wave approximation and putting  $\Delta'_c = \Delta_a = -\omega_m$ , blue detuned laser pulse to both the cavity and atomic resonance, Eq. (14) simplifies to

$$\begin{aligned} \dot{a}_m &= -ig a_c^\dagger, \\ \dot{a}_c &= -\kappa a_c - ig_a c_a - ig a_m^\dagger - \sqrt{2\kappa} a_{in}, \\ \dot{c}_a &= -ig_a a_c, \end{aligned} \quad (15)$$

where, for simplicity of the notation, we have dropped  $\delta$  and the superscripts  $r$  on the displacement operators.

It should be noted from Eq. (15) that there are both, parametric and beam-splitter type of couplings present between the field operators. The coupling between the cavity and mirror field operators is of the parametric type, whereas the coupling between the cavity and atomic field operators is of the beam-splitter type. There is no direct coupling between the mirror and the atomic operators.

### A. Bad cavity limit, $\kappa \gg g, g_a$

The three differential equations (15) can be combined into two if we take the bad cavity limit of  $\kappa \gg g_a, g$ . We can then make an adiabatic approximation  $\dot{a}_c \approx 0$ , and find

$$a_c(t) \approx -i\frac{g_a}{\kappa}c_a(t) - i\frac{g}{\kappa}a_m^\dagger(t) - \sqrt{\frac{2}{\kappa}}a_{\text{in}}(t). \quad (16)$$

When this result is inserted into the remaining two equations  $\dot{a}_m$  and  $\dot{c}_a$  in Eq. (15), we obtain

$$\begin{aligned} \dot{a}_m &= Ga_m + \sqrt{GG_a}c_a^\dagger + i\sqrt{2G}a_{\text{in}}^\dagger, \\ \dot{c}_a^\dagger &= -G_a c_a^\dagger - \sqrt{GG_a}a_m - i\sqrt{2G_a}a_{\text{in}}^\dagger, \end{aligned} \quad (17)$$

where  $G = g^2/\kappa$  and  $G_a = g_a^2/\kappa$ . A direct integration of Eq. (17) yields

$$\begin{aligned} a_m(t) &= a_m(0)e^{Gt} + \sqrt{GG_a}e^{Gt} \int_0^t dt' c_a^\dagger(t')e^{-Gt'} \\ &\quad + i\sqrt{2G}e^{Gt} \int_0^t dt' a_{\text{in}}^\dagger(t')e^{-Gt'}, \end{aligned} \quad (18)$$

$$\begin{aligned} c_a^\dagger(t) &= c_a^\dagger(0)e^{-G_a t} - \sqrt{GG_a}e^{-G_a t} \int_0^t dt' a_m(t')e^{G_a t'} \\ &\quad - i\sqrt{2G_a}e^{-G_a t} \int_0^t dt' a_{\text{in}}^\dagger(t')e^{G_a t'}. \end{aligned} \quad (19)$$

Alternatively, we may write Eq. (17) in a matrix form as

$$\dot{\vec{z}}(t) = \mathbf{M}\vec{z}(t) + i\sqrt{2G}\vec{\eta}(t), \quad (20)$$

where  $\vec{z}(t) = (a_m(t), c_a^\dagger(t))^T$ , the drift matrix  $\mathbf{M}$  is given by

$$\mathbf{M} = G \begin{pmatrix} 1 & \sqrt{\lambda} \\ -\sqrt{\lambda} & -\lambda \end{pmatrix}, \quad (21)$$

and

$$\vec{\eta}(t) = \left( a_{\text{in}}^\dagger(t), -\sqrt{\lambda}a_{\text{in}}^\dagger(t) \right)^T, \quad (22)$$

with  $\lambda = G_a/G$ .

It can be seen from Eq. (21) that the determinant of the matrix  $\mathbf{M}$  is zero. This means that there exists a

linear combination of the operators  $a_m(t)$  and  $c_a^\dagger(t)$  which is a constant of motion.

It is clear from Eq. (17) that a linear combination

$$u(t) = \sqrt{\frac{G_a}{|G-G_a|}}a_m(t) + \sqrt{\frac{G}{|G-G_a|}}c_a^\dagger(t) \quad (23)$$

is a constant of motion,  $\dot{u}(t) = 0$ , that  $u(t)$  does not evolve in time,  $u(t) = u(0)$ . However, there is another linear combination

$$w(t) = \sqrt{\frac{G}{|G-G_a|}}a_m(t) + \sqrt{\frac{G_a}{|G-G_a|}}c_a^\dagger(t), \quad (24)$$

which in the case  $G_a \neq G$  evolves in time. It is easily verified that the linear combinations (23) and (24) satisfy the fundamental commutation relations

$$[[u, u^\dagger]] = [[w, w^\dagger]] = 1, \text{ and } [u, w^\dagger] = 0. \quad (25)$$

We may call the linear combinations  $u(t)$  and  $w(t)$  as superposition modes of the mirror and atomic modes. Since  $u(t)$  is a constant of motion, we see that the evolution of the mode  $w(t)$  completely determines the time evolution of the system.

Let us find the explicit time-dependent behavior of  $w(t)$ . It is not difficult to show from Eq. (17) that the equation of motion for  $w(t)$  depends on whether  $G > G_a$  or  $G_a > G$ . We will consider separately these two cases. For the case  $G > G_a$ , we have

$$\dot{w} = (G - G_a)w + i\sqrt{2(G - G_a)}a_{\text{in}}^\dagger. \quad (26)$$

In its time-integrated form, Eq. (26) is

$$\begin{aligned} w(t) &= w(0)e^{(G-G_a)t} \\ &\quad + i\sqrt{2(G-G_a)}e^{(G-G_a)t} \int_0^t dt' a_{\text{in}}^\dagger(t')e^{-(G-G_a)t'}. \end{aligned} \quad (27)$$

For the case  $G_a > G$ , we have

$$\dot{w} = -(G_a - G)w - i\sqrt{2(G_a - G)}a_{\text{in}}^\dagger, \quad (28)$$

and its time-integrated form is

$$\begin{aligned} w(t) &= w(0)e^{-(G_a-G)t} \\ &\quad - i\sqrt{2(G_a-G)}e^{-(G_a-G)t} \int_0^t dt' a_{\text{in}}^\dagger(t')e^{(G_a-G)t'}. \end{aligned} \quad (29)$$

We may use Eqs. (27) and (29) to evaluate the solutions for  $a_m(t)$  and  $c_a(t)$ . From Eqs. (23) and (24) and for  $G > G_a$ , we have by inversion

$$\begin{aligned} a_m(t) &= -\sqrt{\frac{G_a}{G-G_a}}u(0) + \sqrt{\frac{G}{G-G_a}}w(t), \\ c_a^\dagger(t) &= \sqrt{\frac{G}{G-G_a}}u(0) - \sqrt{\frac{G_a}{G-G_a}}w(t), \end{aligned} \quad (30)$$

which shows that the time evolution of the mirror and atomic field modes is known once  $w(t)$  has been determined from Eq. (27).

Similarly, for  $G_a > G$ , the solutions for  $a_m(t)$  and  $c_a(t)$  are

$$\begin{aligned} a_m(t) &= \sqrt{\frac{G_a}{G_a - G}} u(0) - \sqrt{\frac{G}{G_a - G}} w(t), \\ c_a^\dagger(t) &= -\sqrt{\frac{G}{G_a - G}} u(0) + \sqrt{\frac{G_a}{G_a - G}} w(t), \end{aligned} \quad (31)$$

where in this case  $w(t)$  is given in Eq. (29).

We see that the solutions for  $a_m(t)$  and  $c_a(t)$  are easily written in terms of  $w(t)$  given in Eq. (27) or (29) depending on whether  $G > G_a$  or  $G_a > G$ . Although the solutions for  $w(t)$  in the two cases look very similar, we will see that they lead to quite different results for entanglement between the modes and quantum steering.

## B. Input-output relations

Having the time-dependent solutions for the field operators of the three modes, we may now calculate relations between the input and output amplitudes of the fields. For the cavity field, we use the well known input and output relation

$$a_{\text{out}}^c(t) = a_{\text{in}}(t) + \sqrt{2\kappa} a_c(t), \quad (32)$$

which after applying Eq. (16) becomes

$$\begin{aligned} a_{\text{out}}^c(t) &= -a_{\text{in}}(t) - i\sqrt{2G_a} c_a(t) - i\sqrt{2G_a} a_m^\dagger(t) \\ &= -a_{\text{in}}(t) - i\sqrt{2|G - G_a|} w^\dagger(t). \end{aligned} \quad (33)$$

Since the temporal behavior of  $w(t)$  depends on whether  $G > G_a$  or  $G_a > G$ , we consider the input-output relations separately for those two cases.

### 1. The case $G > G_a$

We first consider the input-output relations in the case  $G > G_a$ . If we insert into Eq. (33) the result for the adjoint of  $w(t)$  from Eq. (27), we obtain

$$\begin{aligned} a_{\text{out}}^c(t) &= -a_{\text{in}}(t) - i\sqrt{2(G - G_a)} w^\dagger(0) e^{(G - G_a)t} \\ &\quad - 2(G - G_a) e^{(G - G_a)t} \int_0^t dt' a_{\text{in}}(t') e^{-(G - G_a)t'}. \end{aligned} \quad (34)$$

It is convenient to introduce a set of normalized temporal light modes

$$\begin{aligned} A_{\text{in}} &= \sqrt{\frac{2(G - G_a)}{1 - e^{-2(G - G_a)\tau}}} \int_0^\tau dt a_{\text{in}}(t) e^{-(G - G_a)t}, \\ A_{\text{out}} &= \sqrt{\frac{2(G - G_a)}{e^{2(G - G_a)\tau} - 1}} \int_0^\tau dt a_{\text{out}}^c(t) e^{(G - G_a)t}, \\ B_{\text{in}} &= a_m(0), \quad B_{\text{out}} = a_m(\tau), \quad C_{\text{in}} = c_a(0), \quad C_{\text{out}} = c_a(\tau), \\ W_{\text{in}} &= w(0), \quad W_{\text{out}} = w(\tau), \quad U_{\text{in}} = u(0), \quad U_{\text{out}} = u(\tau). \end{aligned} \quad (35)$$

By inserting Eqs. (30) and (34) into Eq. (35), we then can determine how the output field of each mode, after an interaction time  $\tau$ , is related to the input fields of the modes involved. After straightforward calculations, we find that the output fields of the three modes are related to the input fields as

$$\begin{aligned} A_{\text{out}} &= -e^{r_\alpha} A_{\text{in}} - i\alpha \sqrt{e^{2r_\alpha} - 1} B_{\text{in}}^\dagger - i\beta \sqrt{e^{2r_\alpha} - 1} C_{\text{in}}, \\ B_{\text{out}} &= (\alpha^2 e^{r_\alpha} - \beta^2) B_{\text{in}} + \alpha\beta (e^{r_\alpha} - 1) C_{\text{in}}^\dagger \\ &\quad + i\alpha \sqrt{e^{2r_\alpha} - 1} A_{\text{in}}^\dagger, \\ C_{\text{out}} &= (\alpha^2 - \beta^2 e^{r_\alpha}) C_{\text{in}} - \alpha\beta (e^{r_\alpha} - 1) B_{\text{in}}^\dagger \\ &\quad + i\beta \sqrt{e^{2r_\alpha} - 1} A_{\text{in}}. \end{aligned} \quad (36)$$

where

$$\alpha = \sqrt{\frac{G}{G - G_a}}, \quad \beta = \sqrt{\frac{G_a}{G - G_a}}, \quad (37)$$

and  $r_\alpha = (G - G_a)\tau = G\tau/\alpha^2$  is the normalized interaction time parameter.

By further expressing the  $B_i$  and  $C_i$  modes in terms of the superposition mode  $W_i$  ( $i = \text{out, in}$ ) stands for the output and input modes), we then find, with the help of Eqs. (24) and (35) that Eq. (36) becomes

$$\begin{aligned} A_{\text{out}} &= -e^{r_\alpha} A_{\text{in}} - i\sqrt{e^{2r_\alpha} - 1} W_{\text{in}}^\dagger, \\ W_{\text{out}} &= e^{r_\alpha} W_{\text{in}} + i\sqrt{e^{2r_\alpha} - 1} A_{\text{in}}^\dagger. \end{aligned} \quad (38)$$

A number of interesting features follow from this equation.

(i) Equation (36) illustrates the intrinsically two-mode behavior of our three mode system that the cavity mode interacts effectively with the superposition mode  $w$  rather than with the mirror and atomic modes separately.

(ii) The system transforms input fields into the output fields with a real amplitude  $e^{r_\alpha}$  that for  $G > G_a$  is greater than one. Thus, the system might reasonably be called as an amplifier with the gain factor  $e^{r_\alpha}$ . It is particularly well seen when one calculates the average number of photons in the output modes. By using Eq. (10) for the correlations in the input fields, we readily find

$$\begin{aligned} n_c(\tau) &= \langle A_{\text{out}}^\dagger A_{\text{out}} \rangle = \alpha^2 (n_0 + 1) (e^{2r_\alpha} - 1), \\ n_w(\tau) &= \langle W_{\text{out}}^\dagger W_{\text{out}} \rangle = \alpha^2 (n_0 + 1) e^{2r_\alpha} - 1. \end{aligned} \quad (39)$$

We see that the average number of photons in both modes increases with  $r$  that the output fields are amplified during the evolution process. Note the conservation of the difference between the average number of photons in the two modes,  $n_w(\tau) - n_c(\tau) = n_w(0)$ , characteristic for parametric amplification.

(iii) The parameter  $r_\alpha$  depends on the difference  $G - G_a$  rather than the sum  $G + G_a$  of the coupling strengths. This is connected with the presence of two different types of couplings between the modes, the parametric coupling between the cavity and the mirror modes described by  $G$ , and the beam-splitter type coupling between the cavity and the atomic modes described by  $G_a$ . The parametric coupling creates squeezing (correlations) between the mirror and cavity modes to a degree  $G\tau$  that then with a degree  $G_a\tau$  is transferred to the atomic mode. Thus, the effective strength of the parametric interaction between the modes is  $(G - G_a)\tau$ . It is easy to understand if one notices that the superposition mode  $w$  is a combination of the operators characteristics of a two-mode squeezed state. Noting from Eq. (37) that

$$\alpha = \cosh s, \quad \beta = \sinh s, \quad (40)$$

where  $s = \text{arctanh} \sqrt{G_a/G}$ , it then follows from Eq. (24) that

$$w = a_m \cosh s + c_a^\dagger \sinh s = S(s)a_m S^\dagger(s). \quad (41)$$

Clearly,  $w$  is the annihilation operator of a combination of two field modes in which the annihilation operator mirror mode is couple to the Hermitian conjugate of the atomic mode. Such a combination is generated by the squeezing transformation of the annihilation operator  $a_m$  with the unitary two-mode squeeze operator

$$S(s) = e^{s(a_m c_a - a_m^\dagger c_a^\dagger)}. \quad (42)$$

Evidently, the superposition (41) results from a two-mode squeezing transformation with the two-mode squeezing parameter  $s$ .

(iv) The appearance of the two-mode squeezed state (41) is a surprising result since according to Eq. (15), the mirror and the atoms are not coupled through a parametric process. This type of coupling is created dynamically by the fast decaying cavity mode. The parametric coupling between the cavity and the mirror creates a two-mode squeezed state between  $a_m$  and  $a_c$  modes. Due to the fast damping of the cavity mode, the beam-splitter type coupling between  $a_c$  and  $c_a$  swaps the cavity mode with the atomic mode to form the superposition mode  $w$ .

(v) Equation (40) shows that the ratio  $G_a/G$  determines the degree of squeezing (correlation) between the mirror and the atoms. When  $G_a \rightarrow G$ , the squeezing parameter  $s \rightarrow \infty$ , and then the modes  $a_m$  and  $c_a$ , which form the combination  $w$ , become themselves maximally squeezed or, equivalently, maximally entangled. Simultaneously, when  $s$  increases the squeezing parameter  $r_\alpha$  decreases, indicating that the squeezing processes determined by the parameters  $s$  and  $r_\alpha$  exclude

each other. The simplest way to identify the competition between these two squeezing processes is to test the Cauchy-Schwarz inequality. Two modes are said to be squeezed if the Cauchy-Schwarz inequality is violated. It is well known that in the case of a Gaussian state, the Cauchy-Schwarz inequality is violated when the anomalous cross-correlation function

$$\eta = \frac{|\langle A_{\text{out}}(\tau) W_{\text{out}}(\tau) \rangle|^2}{n_c(\tau) n_w(\tau)} \quad (43)$$

is larger than one. Using Eqs. (36) and (39), we find

$$\eta = \frac{(n_0 + 1)e^{2r_\alpha} \cosh^2 s}{(n_0 + 1)e^{2r_\alpha} \cosh^2 s - 1}. \quad (44)$$

Evidently,  $\eta > 1$  for any  $r_\alpha$  and  $s$  except for  $s \rightarrow \infty$ , at which  $\eta$  approaches no squeezing limit ( $\eta = 1$ ) irrespective of  $r_\alpha$ . Viewed as a function of  $s$ , the cross-correlation function  $\eta$  is largest for  $s = 0$  and decreases with an increasing  $s$ . From this it follows that the modes  $a_c$  and  $w$  can be squeezed as long as  $s < \infty$  and the squeezing vanishes in the limit of  $s \rightarrow \infty$ . On the other hand, at  $s \rightarrow \infty$ , the modes  $a_m$  and  $c_a$ , which form the combination  $w$ , are themselves maximally squeezed. Hence, in our three-mode system with  $G > G_a$ , squeezing can occur between the cavity mode and the combination  $w$  of the modes  $a_m$  and  $c_a$  if those modes are *not* themselves maximally squeezed. We shall return to this problem in more details in Sec. III and IV, where we examine entanglement and quantum steering between different combinations of the modes.

## 2. The case $G_a > G$

A calculation similar to that of the case  $G > G_a$  can be applied to find the input-output relations for the case  $G_a > G$ . As in the previous case, we determine the time evolution of the field operators in terms of  $w(t)$ , which in the present case is given by Eq. (29). First, we evaluate the output cavity field from the expression (33) and by using Eq. (29), we find

$$a_{\text{out}}^c(t) = -a_{\text{in}}(t) - i\sqrt{2(G_a - G)}w^\dagger(0)e^{-(G_a - G)t} + 2(G_a - G)e^{-(G_a - G)t} \int_0^t dt' a_{\text{in}}(t')e^{(G_a - G)t'}. \quad (45)$$

In analogy to the previous case, we define a set of the normalized modes

$$A_{\text{in}} = \sqrt{\frac{2(G_a - G)}{e^{2(G_a - G)\tau} - 1}} \int_0^\tau dt a_{\text{in}}(t)e^{(G_a - G)t},$$

$$A_{\text{out}} = \sqrt{\frac{2(G_a - G)}{1 - e^{-2(G_a - G)\tau}}} \int_0^\tau dt a_{\text{out}}^c(t)e^{-(G_a - G)t},$$

$$B_{\text{in}} = a_m(0), \quad B_{\text{out}} = a_m(\tau), \quad C_{\text{in}} = c_a(0), \quad C_{\text{out}} = c_a(\tau),$$

$$W_{\text{in}} = w(0), \quad W_{\text{out}} = w(\tau), \quad U_{\text{in}} = u(0), \quad U_{\text{out}} = u(\tau), \quad (46)$$

and find that the output fields of the individual modes can be expressed in terms of the input fields as

$$\begin{aligned}
A_{\text{out}} &= -e^{-r'_\beta} A_{\text{in}} - i\beta' \sqrt{1 - e^{-2r'_\beta}} B_{\text{in}}^\dagger \\
&\quad - i\alpha' \sqrt{1 - e^{-2r'_\beta}} C_{\text{in}}, \\
B_{\text{out}} &= \left(\alpha'^2 - \beta'^2 e^{-r'_\beta}\right) B_{\text{in}} + \alpha' \beta' \left(1 - e^{-r'_\beta}\right) C_{\text{in}}^\dagger \\
&\quad + i\beta' \sqrt{1 - e^{-2r'_\beta}} A_{\text{in}}^\dagger, \\
C_{\text{out}} &= \left(\alpha'^2 e^{-r'_\beta} - \beta'^2\right) C_{\text{in}} - \alpha' \beta' \left(1 - e^{-r'_\beta}\right) B_{\text{in}}^\dagger \\
&\quad + i\alpha' \sqrt{1 - e^{-2r'_\beta}} A_{\text{in}}, \tag{47}
\end{aligned}$$

where

$$\alpha' = \sqrt{\frac{G_a}{G_a - G}}, \quad \beta' = \sqrt{\frac{G}{G_a - G}}, \tag{48}$$

and  $r'_\beta = G\tau/\beta'^2 = r/\beta'^2$ .

By introducing the superposition mode  $W_i$ , the input-output relations (47) simplify to

$$\begin{aligned}
A_{\text{out}} &= -e^{-r'_\beta} A_{\text{in}} - i\sqrt{1 - e^{-2r'_\beta}} W_{\text{in}}^\dagger, \\
W_{\text{out}} &= e^{-r'_\beta} W_{\text{in}} - i\sqrt{1 - e^{-2r'_\beta}} A_{\text{in}}^\dagger. \tag{49}
\end{aligned}$$

We see that similar to the  $G > G_a$  case, the system effectively behaves as a two-mode system. However, there are two important differences from the  $G > G_a$  case.

(i) The system transforms input fields into the output fields with an amplitude which falls off exponentially with the parameter  $r'_\beta$ . Therefore, for  $G_a > G$  the system behaves like an attenuator. This can be seen by considering the average number of photons in the output modes. With the help of Eq. (10), the average numbers of photons in the modes evaluated from Eq. (49) are

$$\begin{aligned}
n_c(\tau) &= \beta'^2 (n_0 + 1) \left(1 - e^{-2r'_\beta}\right), \\
n_w(\tau) &= \beta'^2 (n_0 + 1) e^{-2r'_\beta} + 1. \tag{50}
\end{aligned}$$

Unlike the  $G > G_a$  case, the number of photons in the cavity mode increases with an increasing  $r'_\beta$  in expense of a decreasing number of photons in the modes  $w$  and saturates at  $n_c(\infty) = \beta'^2 (n_0 + 1)$ . Note the conservation of the sum of the number of photons,  $n_c(\tau) + n_w(\tau) = n_w(0)$ . This implies that in the present case, the effective coupling between the modes is of the form of beam-splitter process.

(ii) A consequence of the beam-splitter coupling between the modes is no squeezing between the  $a_c$  and  $w$  modes. It is easy to show. When Eqs. (49) and (50) are applied into Eq. (43), we find that

$$\eta = \frac{\beta'^2 (n_0 + 1) e^{-2r'_\beta}}{\beta'^2 (n_0 + 1) e^{-2r'_\beta} + 1}. \tag{51}$$

This shows that always  $\eta < 1$ . It then follows that the Cauchy-Schwarz inequality cannot be violated and consequently no squeezing between the modes. However, it does not mean that squeezing or, equivalently, entanglement cannot occur between combinations of other modes of the system. We shall examine the possibility for entanglement between different combinations of the modes in Sec. III.

### C. Quadrature components

The information about entanglement between modes is obtained by studying the variances of the quadrature components of the fields and their linear combinations. To do that, we introduce the standard definitions of the in-phase  $X$  and out-of-phase  $P$  quadrature components

$$X_A^i = \frac{1}{\sqrt{2}} [A^i + (A^i)^\dagger], \quad P_A^i = \frac{1}{\sqrt{2}i} [A^i - (A^i)^\dagger], \tag{52}$$

where  $A$  denotes the annihilation operator of a particular field mode,  $A = (a_c, a_m, c_a)$ , and "i" stands for the output and input modes,  $i = (\text{out}, \text{in})$ .

The general expressions for the relations between the quadratures of the input and output fields are quite lengthy, and are listed in the Appendix. We proceed here with the relations between the quadrature components of the cavity mode and the superposition modes  $w$  and  $u$ , which are convenient to study the variances of the quadrature components and their properties.

In the case with  $G > G_a$ , we introduce quadrature components for the input and output fields of the superposition modes

$$\begin{aligned}
X_w^i &= \alpha X_m^i + \beta X_c^i, & P_w^i &= \alpha P_m^i - \beta P_c^i, \\
X_u^i &= \beta X_m^i + \alpha X_c^i, & P_u^i &= \beta P_m^i - \alpha P_c^i, \tag{53}
\end{aligned}$$

and find that the output-input relations, Eqs. (A1) and (A2), simplify to

$$\begin{aligned}
X_a^{\text{out}} &= -e^{r_\alpha} X_a^{\text{in}} - \sqrt{e^{2r_\alpha} - 1} P_w^{\text{in}}, \\
X_w^{\text{out}} &= e^{r_\alpha} X_w^{\text{in}} + \sqrt{e^{2r_\alpha} - 1} P_a^{\text{in}}, \\
X_u^{\text{out}} &= X_u^{\text{in}}, \tag{54}
\end{aligned}$$

and

$$\begin{aligned}
P_a^{\text{out}} &= -e^{r_\alpha} P_a^{\text{in}} - \sqrt{e^{2r_\alpha} - 1} X_w^{\text{in}}, \\
P_w^{\text{out}} &= e^{r_\alpha} P_w^{\text{in}} + \sqrt{e^{2r_\alpha} - 1} X_a^{\text{in}}, \\
P_u^{\text{out}} &= P_u^{\text{in}}. \tag{55}
\end{aligned}$$

Similarly, in the case with  $G_a > G$ , by introducing quadrature components

$$\begin{aligned}
X_{w'}^i &= \beta' X_m^i + \alpha' X_c^i, & P_{w'}^i &= \beta' P_m^i - \alpha' P_c^i, \\
X_{u'}^i &= \alpha' X_m^i + \beta' X_c^i, & P_{u'}^i &= \alpha' P_m^i - \beta' P_c^i, \tag{56}
\end{aligned}$$

we find from Eqs. (A3) and (A4) that

$$\begin{aligned} X_a^{\text{out}} &= -e^{-r'_\beta} X_a^{\text{in}} - \sqrt{1 - e^{-2r'_\beta}} P_{w'}^{\text{in}}, \\ X_{w'}^{\text{out}} &= e^{-r'_\beta} X_{w'}^{\text{in}} - \sqrt{1 - e^{-2r'_\beta}} P_a^{\text{in}}, \\ X_{u'}^{\text{out}} &= X_{u'}^{\text{in}}, \end{aligned} \quad (57)$$

and

$$\begin{aligned} P_a^{\text{out}} &= -e^{-r'_\beta} P_a^{\text{in}} - \sqrt{1 - e^{-2r'_\beta}} X_{w'}^{\text{in}}, \\ P_{w'}^{\text{out}} &= e^{-r'_\beta} P_{w'}^{\text{in}} - \sqrt{1 - e^{-2r'_\beta}} X_a^{\text{in}}, \\ P_{u'}^{\text{out}} &= P_{u'}^{\text{in}}. \end{aligned} \quad (58)$$

Note that the  $X^{\text{out}}$  quadrature component of a given output field depends on the  $P^{\text{in}}$  component of the other input field, and vice versa,  $P^{\text{out}}$  component of a given output field depends on the  $X^{\text{in}}$  component of the other field. This clearly indicates the possibility for entanglement in the  $X - P$  combination of the modes  $a_c$  and  $w$ . Generally speaking, there are three different types of possible combinations of the modes,  $X - X$ ,  $X - P$  and  $P - P$ , which can be considered when searching for entanglement between the modes.

#### D. Large squeezing regime, $r_\alpha, r'_\beta \gg 1$ .

Before moving on to consideration of the variances of the quadrature components, it is worthwhile to look at properties of the quadratures in the limit of a large squeezing,  $r_\alpha, r'_\beta \rightarrow \infty$ . As we have already mentioned, the presence of the  $X - P$  type coupling between the quadratures suggests a possibility for EPR correlations between the  $a_c$  and  $w$  modes. It can be seen when one takes the limit of a large squeezing,  $r_\alpha \rightarrow \infty$ . In the amplification regime,  $G > G_a$ , by taking  $r_\alpha \rightarrow \infty$  in Eqs. (54) and (55), and comparing the resulting expressions for  $X_a^{\text{out}}$  and  $P_w^{\text{out}}$ , we find

$$X_a^{\text{out}} = -P_w^{\text{out}}. \quad (59)$$

This demonstrates the possibility of a perfect EPR correlation between the modes that independent of the state of the input fields, the  $P_w^{\text{out}}$  component of the mode  $w$  can be predicted with certainty from a measurement of the  $X_a^{\text{out}}$  component of the cavity field.

However, if we consider relations between quadrature components of the three output fields of the system, we find

$$\begin{aligned} X_a^{\text{out}} &= -\frac{1}{\beta} P_c^{\text{out}}, & P_a^{\text{out}} &= \frac{1}{\beta} X_c^{\text{out}}, \\ X_a^{\text{out}} &= -\frac{1}{\alpha} P_m^{\text{out}}, & P_a^{\text{out}} &= -\frac{1}{\alpha} X_m^{\text{out}}, \\ X_c^{\text{out}} &= -\frac{\beta}{\alpha} X_m^{\text{out}}, & P_c^{\text{out}} &= \frac{\beta}{\alpha} P_m^{\text{out}}. \end{aligned} \quad (60)$$

This shows that as long as the three modes are involved ( $\alpha > 1, \beta \neq 0$ ), only imperfect EPR correlations can be created between the output modes at  $r_\alpha \rightarrow \infty$ . In other words, from a measurement of one of the quadratures, for example,  $X_a^{\text{out}}$ , we can infer only a partial information about the quadratures  $P_c^{\text{out}}$  and  $P_m^{\text{out}}$ . This is because the mirror and the atoms are coupled to the cavity mode with unequal strengths,  $G$  and  $G_a$ , respectively. In physical terms, the unequal coupling results in a partial distinguishability of the modes. It is interesting that even if there are imperfect EPR correlations between any pair of the individual modes, there exists the linear combination  $w$  of the mirror and atomic modes which exhibits a perfect EPR correlation with the cavity mode.

The situation differs in the case of attenuation,  $G_a > G$ . In this case, by taking the limit  $r'_\beta \rightarrow \infty$  in Eqs. (57) and (58), one finds

$$\begin{aligned} X_a^{\text{out}} &= -P_{w'}^{\text{in}}, & X_{w'}^{\text{out}} &= P_a^{\text{in}}, \\ P_a^{\text{out}} &= -X_{w'}^{\text{in}}, & P_{w'}^{\text{out}} &= -X_a^{\text{in}}. \end{aligned} \quad (61)$$

We see that in this case, a state transfer or, equivalently, state swapping effect occurs between the input and output modes rather than the creation of entanglement between the output modes. The in-phase (out-of-phase) quadrature component of a given input field is transferred into the out-of-phase (in-phase) component of the output field of the other mode. Thus, in the limit of  $r'_\beta \rightarrow \infty$  no entanglement is created between the modes  $a_c$  and  $w$ . Nevertheless, we will demonstrate that there is still possible to create EPR type correlations between some combinations of the modes.

### III. BIPARTITE ENTANGLEMENT

Our interest is in the creation of entanglement, in particular, perfect EPR entangled states between the modes of the three-mode optomechanical system. The entanglement is associated with correlations between the modes which are reflected in the variances in linear combinations of the quadrature components of the modes. To quantify entanglement, we use the DGCZ criterion [29] and asymmetric criterion [27, 30, 31] for the variances of symmetric and asymmetric combinations of the quadrature components of the field modes. We consider different combinations,  $X - X$ ,  $X - P$  and  $P - P$  of the in-phase and out-of-phase quadrature components of the modes.

#### A. Symmetric entanglement criteria

Let us first consider the DGCZ inseparability criterion for the symmetric  $X - P$  combinations of the quadrature components of the output fields. This is quantified with the inseparability parameter

$$\Delta_{i,j} = [\Delta (X_i^{\text{out}} \pm P_j^{\text{out}})]^2 + [\Delta (P_i^{\text{out}} \pm X_j^{\text{out}})]^2, \quad (62)$$



where  $i, j = a, m, c, w$ , and  $j \neq i$ . Two modes  $i$  and  $j$  are said to be entangled iff  $\Delta_{i,j} < 2$ .

For the input fields we assume that the cavity and atomic modes are in the ordinary vacuum state whereas the mirror field mode is in a thermal state with occupation number  $n_0$ . Then the variances of the input fields in the modes  $w$  and  $u$  are

$$\begin{aligned} (\Delta X_w^{\text{in}})^2 &= (\Delta P_w^{\text{in}})^2 = \alpha^2 \left( n_0 + \frac{1}{2} \right) + \frac{1}{2} \beta^2, \\ (\Delta X_u^{\text{in}})^2 &= (\Delta P_u^{\text{in}})^2 = \beta^2 \left( n_0 + \frac{1}{2} \right) + \frac{1}{2} \alpha^2. \end{aligned} \quad (63)$$

We focus first on the case  $G > G_a$  and calculate all the possible two-mode variances  $\Delta_{i,j}$ . When Eqs. (53)-(54) are used in Eq. (62), we readily find the general expressions for the inseparability parameter  $\Delta_{i,j}$  of the symmetric  $X - P$  combinations

$$\begin{aligned} \Delta_{a,c} &= 2 + 2\alpha^2 (n_0 + 1) \left[ e^{2r\alpha} - 1 + \beta^2 (e^{r\alpha} - 1)^2 \right], \\ \Delta_{m,c} &= 2 (n_0 + 1) \left[ (\alpha^2 e^{r\alpha} - \beta^2)^2 + \alpha^2 \beta^2 (e^{r\alpha} - 1)^2 \right], \\ \Delta_{a,m} &= 2 (n_0 + 1) \left[ \alpha \left( \alpha e^{r\alpha} - \sqrt{e^{2r\alpha} - 1} \right) - \beta^2 \right]^2. \end{aligned} \quad (64)$$

Had we considered only the mirror coupled to the cavity mode, ( $\alpha = 1, \beta = 0$ ), the parameter  $\Delta_{a,m}$  would have been

$$\Delta_{a,m} = 2(n_0 + 1) \left( e^r - \sqrt{e^{2r} - 1} \right)^2, \quad (65)$$

with  $r = G\tau$ , which is the result of Hofer *et al.* [26], who considered EPR entanglement in a two-mode optomechanical system.

It is easily verified from Eq. (64) that among the three parameters determining bipartite correlations between the modes only  $\Delta_{a,m}$  can be reduced below the separability level 2. At  $\tau = 0$  ( $r_\alpha = 0$ ) the modes are separable and immediately afterwards,  $\Delta_{a,c}$  and  $\Delta_{m,c}$  begin to increase whereas  $\Delta_{a,m}$  decreases below 2. This is shown in Fig. 2, where we plot  $\Delta_{a,m}$  as a function of  $r$  for several different values of  $\alpha$ . For  $\alpha = 1$ , the parameter  $\Delta_{a,m}$  decreases with an increasing  $r$  and at  $r \rightarrow \infty$ ,  $\Delta_{a,m} \rightarrow 0$  indicating that the state of the two modes becomes a perfect EPR state. However, as the coupling  $\alpha$  increases,  $\Delta_{a,m}$  rapidly increases at large  $r$  and becomes greater than 2. Thus, for  $\alpha > 1$  entanglement occurs in a restricted range of  $r$  that only at small  $r$  the entanglement survives. Hence, for  $\alpha > 1$  the state is not a perfect EPR state.

Although the perfect EPR state between the modes  $a_c$  and  $a_m$  disappears when  $\alpha > 1$ , it must not be thought that then there is no possibility to create a perfect EPR state in the system. When  $\alpha > 1$ , the perfect EPR state is still there, but it is between the cavity mode  $a_c$  and the superposition mode  $w$ . When we calculate the parameter  $\Delta_{a,w}$ , we find

$$\Delta_{a,w} = 2\alpha^2 (n_0 + 1) \left( e^{r\alpha} - \sqrt{e^{2r\alpha} - 1} \right)^2. \quad (66)$$

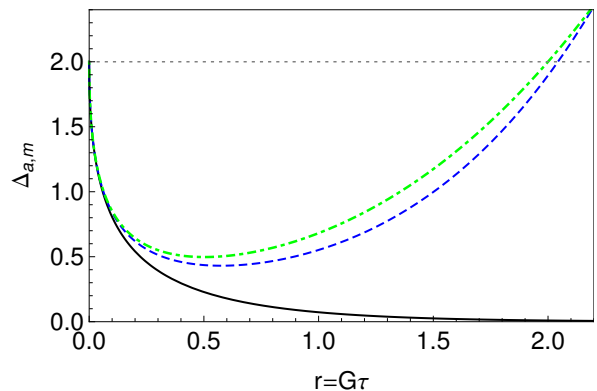


Figure 2: (Color online) Variation of the inseparability parameter  $\Delta_{a,m}$  with  $r = G\tau$  for  $n_0 = 0$  and several different values of  $\alpha$ :  $\alpha = 1$  (solid black),  $\alpha = 2$  (dashed blue),  $\alpha = 10$  (dot-dashed green).

Apart from the appearance of the factor  $\alpha^2$ , Eq. (66) is formally identical with the result given in Eq. (65) for the two-mode optomechanical system. The system evidently tends to behave as a two-mode system. Therefore,  $\Delta_{a,w}$  too gets reduced below 2 and tends to zero when  $r \rightarrow \infty$ . Thus, a perfect EPR state can be created in the system even if  $\alpha > 1$ . Since  $\alpha \geq 1$ , it is clear that the entanglement between  $a_c$  and  $w$  occurs in a more restricted range of  $r$  than that predicted for the two-mode optomechanical system. In the presence of the thermal noise ( $n_0 \neq 0$ ), the entanglement occurs in a more restricted area and its magnitude also drops further. It is worth noting that the effect of the thermal noise on the parameters  $\Delta_{i,j}$  is merely to increase their magnitudes by a factor  $(n_0 + 1)$ .

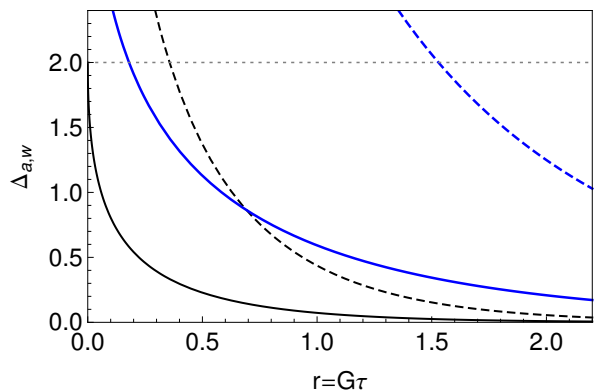


Figure 3: (Color online) Variation of the parameter  $\Delta_{a,w}$  with  $r = G\tau$  for several different values of  $n_0$  and  $\alpha$ . Lower solid black line for  $n_0 = 0, \alpha = 1$ . Lower dashed black line for  $n_0 = 5, \alpha = 1$ . Upper solid blue line for  $n_0 = 0, \alpha = 1.5$ . Upper dashed blue line for  $n_0 = 5, \alpha = 1.5$ . Dotted line indicates position of  $\Delta_{a,w} = 2$ , the threshold for entanglement.

To illustrate the behavior discussed above we show in Fig. 3 the parameter  $\Delta_{a,w}$  as a function of  $r$  for several different values of  $n_0$  and  $\alpha$ . For  $n_0 = 0$  and  $\alpha = 1$ ,

entanglement is seen to occur over the entire range of  $r$  and the created state approaches an EPR state,  $\Delta_{a,w} \rightarrow 0$  as  $r \rightarrow \infty$ . For  $n_0 > 0$  entanglement occurs in the reduced range of  $r$ :

$$r > r_0 = \alpha^2 \ln \frac{\alpha^2(n_0 + 1) + 1}{2\alpha\sqrt{n_0 + 1}}. \quad (67)$$

It then follow from  $r = G\tau$  that  $\Delta_{a,w} < 2$  everywhere except during the short interaction time. Thus we see that the principal effect of thermal photons and the addition of the third mode is to add the initial noise which delays the creation of entanglement to longer interaction times. Comparing the behavior of  $\Delta_{a,w}$  with  $\Delta_{a,m}$ , we may conclude that with an increasing  $\alpha$ , the entanglement between the modes  $a_c$  and  $a_m$  is transferred to the modes  $a_c$  and  $w$ . This conclusion is entirely consistent with the conclusions reached earlier in Sec. IID that for  $\alpha > 1$ , perfect EPR correlations are created only between the cavity mode  $a_c$  and the superposition mode  $w$ .

Turning now to the case  $G_a > G$ , we find with the help of the output-input relations, Eqs. (56)-(58), that

$$\begin{aligned} \Delta_{a,c} &= 2 + 2\beta'^2 (n_0 + 1) \left[ 1 - e^{-2r'_\beta} + \alpha'^2 \left( 1 - e^{-r'_\beta} \right)^2 \right], \\ \Delta_{m,c} &= 2(n_0 + 1) \left[ \left( \alpha'^2 - \beta'^2 e^{-r'_\beta} \right)^2 + \alpha'^2 \beta'^2 \left( 1 - e^{-r'_\beta} \right)^2 \right], \\ \Delta_{a,m} &= 2(n_0 + 1) \left[ \alpha'^2 - \beta' \left( \beta' e^{-r'_\beta} + \sqrt{1 - e^{-2r'_\beta}} \right) \right]^2, \end{aligned} \quad (68)$$

and

$$\Delta_{a,w} = 2 + 2\beta'^2 (n_0 + 1) \left( e^{-r'_\beta} + \sqrt{1 - e^{-2r'_\beta}} \right)^2. \quad (69)$$

Equations (68) and (69) are markedly different from Eqs. (64) and (65), their counterparts for the case  $G > G_a$ . First of all,  $\Delta_{a,w}$  is always greater than 2, and among the other parameters only  $\Delta_{a,m}$  can be reduced below 2. Consequently, entanglement can be created only between the cavity mode and the mirror. This indicates that in contrast to the case  $G > G_a$ , the cavity mode entangles with the mirror alone rather than with the mode  $w$  which is the superposition of the mirror and atomic modes.

The behavior of  $\Delta_{a,m}$  given by Eq. (68) is illustrated in Fig. 4 for  $n_0 = 0$  and for several different values of  $\alpha'$ . For  $\alpha' < \sqrt{2}$ , which corresponds to  $G < G_a/2$ , entanglement is seen to occur over the entire range of  $r$ . For  $\alpha' > \sqrt{2}$ , entanglement occurs only in the restricted range of  $r$ , but it is accompanied by an enhancement in the degree of entanglement. It is interesting that the smaller parametric coupling strength  $G$  produces entanglement at larger range of  $r$  than the larger  $G$  does. It turns out that the smallest value of  $\Delta_{a,m}$ , corresponding to optimum entanglement, is achieved when  $\alpha' \gg 1$ , in which case  $\Delta_{a,m} = 1/2$ . Hence, we may speak of 75% entanglement. It follows that the entanglement is not

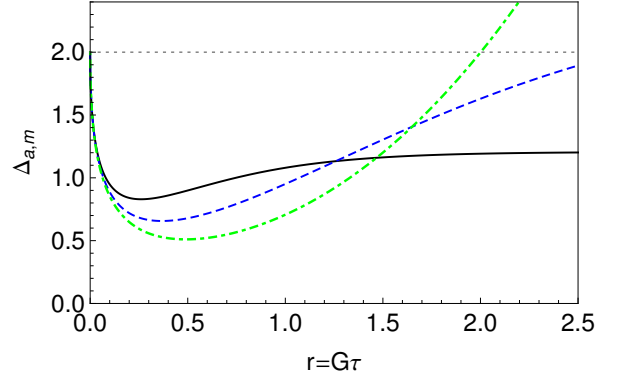


Figure 4: (Color online) Variation of the parameter  $\Delta_{a,m}$  with  $r = G\tau$  for the case  $G_a > G$ ,  $n_0 = 0$  and several values of  $\alpha'$ :  $\alpha' = 1.2$  (solid black),  $\alpha' = 1.5$  (dashed blue),  $\alpha' = 5$  (dot-dashed green).

perfect, so that the state corresponding to the maximum entanglement is not an EPR state.

We have already noticed an important difference between the two cases  $G > G_a$  and  $G_a > G$  that in the case with  $G_a > G$  there is no entanglement between the cavity mode and the superposition mode  $w$ . This conclusion is evident from Eq. (69), which clearly shows that  $\Delta_{a,w}$  cannot be reduced below 2. This could suggest that in the case with  $G_a > G$ , the beamsplitter type coupling between the cavity mode and the atoms destroys the entanglement already created between the cavity mode and the mirror. In fact, the entanglement is not destroyed, it is still there but occurs between the mirror and the atoms. To see this, we evaluate the separability criterion for the  $X_m^{\text{out}} + X_c^{\text{out}}$  and  $P_m^{\text{out}} - P_c^{\text{out}}$  combinations of the quadrature components

$$\Upsilon_{m,c} = [\Delta (X_m^{\text{out}} + X_c^{\text{out}})]^2 + [\Delta (P_m^{\text{out}} - P_c^{\text{out}})]^2. \quad (70)$$

The reason we evaluate variances of the  $X-X$  and  $P-P$  combinations rather than that for  $X-P$  combinations is in the relation between the input-output quadrature components of the mirror and atomic fields. According to Eqs. (A3) and (A4), the in-phase quadrature components of the  $a_m$  and  $a_c$  modes are coupled to the in-phase quadrature components of the input fields. The same property is seen for the out-of-phase quadrature components. Thus, using Eqs. (A3) and (A4) in Eq. (70), we readily find

$$\Upsilon_{m,c} = 2(n_0 + 1) \left[ 1 - \frac{\beta' (1 - e^{-r'_\beta})}{\alpha' + \beta'} \right]^2. \quad (71)$$

It is clear from Eq. (71) that  $\Upsilon_{m,c}$  can be reduced below 2, but only if  $r'_\beta$  and  $\beta'$  are both different from zero. Since  $\beta' \neq 0$  when  $G \neq 0$ , it follows that the presence of the parametric coupling between the mirror and the cavity mode is necessary for entanglement between the mirror

and the atoms. We may find the minimum value of  $\Upsilon_{m,c}$ . In the limit of  $r \rightarrow \infty$ , the parameter  $\Upsilon_{m,c}$  reduces to

$$\Upsilon_{m,c} = 2(n_0 + 1) \left[ \frac{\alpha'}{\alpha' + \beta'} \right]^2. \quad (72)$$

The minimum value of  $\Upsilon_{m,c}$ , corresponding to maximum entanglement between the mirror and the atoms, is reached when  $\alpha', \beta' \gg 1$ , in which case  $\Upsilon_{m,c} = (n_0 + 1)/2$ . It follows that the maximum 75% entanglement can be achieved when  $n_0 = 0$ .

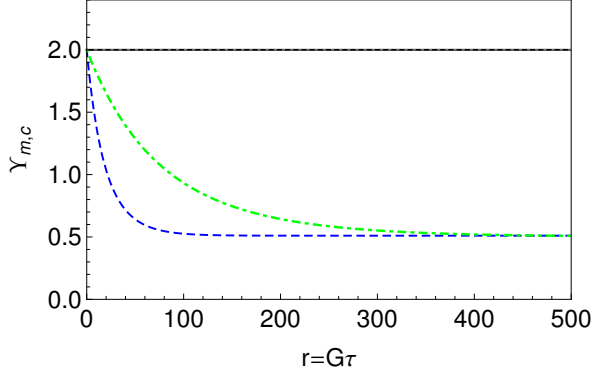


Figure 5: (Color online) Variation of the parameter  $\Upsilon_{m,c}$  with  $r = G\tau$  for the case  $G_a > G$ ,  $n_0 = 0$  and several values of  $\alpha'$ :  $\alpha' = 1$  (solid black),  $\alpha' = 5$  (dashed blue),  $\alpha' = 10$  (dot-dashed green).

The above considerations are illustrated in Fig. 5, which shows  $\Upsilon_{m,c}$  as a function of  $r = G\tau$  for different values of  $\alpha'$ . When  $\alpha' \neq 1$ , corresponding to  $G \neq 0$ , the entanglement is seen to occur over the entire range of  $r$ . It is apparent that the entanglement increases with an increasing  $r$  and that when  $\alpha' \gg 1$ , the optimum entanglement of  $\Upsilon_{m,c} = 1/2$  is achieved at  $r \rightarrow \infty$ .

## B. Asymmetric entanglement criteria

A close look at the output-input relations between the quadrature components, Eqs. (A1)-(A4) in the Appendix, reveals that symmetric combinations of the output fields are accompanied by asymmetric rather than symmetric combinations of the input fields. These asymmetries arise not only from a difference between the coupling strengths  $G$  and  $G_a$  but also from the presence of the thermal noise only at the mirror. This suggests that symmetric combinations of the output fields may not be able to detect the presence of an entanglement between modes that might be present in an asymmetric combination. For this reason, we now consider the criterion for asymmetric combinations of the quadrature components [27], in particular, to see if we can find an entanglement between the mirror and the atoms which, as we have seen in Eq. (15), are not directly coupled to each other.

The inseparability criterion for asymmetric  $X-P$  combinations of the quadrature components of the output

modes  $i$  and  $j$  is confirmed when

$$[\Delta(X_i^{\text{out}} + gP_j^{\text{out}})]^2 + [\Delta(P_i^{\text{out}} + gX_j^{\text{out}})]^2 < 1 + g^2, \quad (73)$$

where  $g$  is a weight factor which is chosen to minimize the variances. The value of  $g$  which minimizes  $\Delta_{a,m}^g$  is easily found using the variational method. By taking the derivative of  $\Delta_{a,m}^g$  over  $g$  and setting  $\partial\Delta_{a,m}^g/\partial g = 0$ , we arrive to a quadratic equation for  $g$  whose the roots can be expressed as

$$g = \frac{-b \pm \sqrt{b^2 - 4ac}}{2a}, \quad (74)$$

where  $b = (\Delta P_m^{\text{out}})^2 - (\Delta X_a^{\text{out}})^2$  and  $c = -a = \langle X_a^{\text{out}} P_m^{\text{out}} \rangle$ . We then choose the root which minimizes  $\Delta_{a,m}^g$ .

A close look at Eqs. (A1)-(A4) in the Appendix reveals the following properties of the cross correlations between the modes

$$\begin{aligned} \langle X_a^{\text{out}} P_c^{\text{out}} \rangle &= \langle P_c^{\text{out}} X_a^{\text{out}} \rangle \\ &= -\langle P_a^{\text{out}} X_c^{\text{out}} \rangle = -\langle X_c^{\text{out}} P_c^{\text{out}} \rangle, \\ \langle X_m^{\text{out}} P_c^{\text{out}} \rangle &= \langle P_c^{\text{out}} X_m^{\text{out}} \rangle \\ &= \langle P_m^{\text{out}} X_c^{\text{out}} \rangle = \langle X_c^{\text{out}} P_m^{\text{out}} \rangle = 0. \end{aligned} \quad (75)$$

Then, it is easily verified that the left side of the inequality (73) for the combinations of the modes  $a-c$  and  $m-c$  becomes

$$(\Delta X_{a,m}^{\text{out}})^2 + (\Delta P_{a,m}^{\text{out}})^2 + g^2[(\Delta X_c^{\text{out}})^2 + (\Delta P_c^{\text{out}})^2], \quad (76)$$

which is always greater than the right side  $1 + g^2$ .

Entanglement is possible the asymmetric  $X-P$  combinations of the quadrature components of the modes  $a$  and  $m$ . Further, using the argument that the output quadrature  $X_m^{\text{out}}$  is related to the input quadrature  $X_c^{\text{in}}$  and vice versa, the output quadrature  $X_c^{\text{out}}$  is related to the input quadrature  $X_m^{\text{in}}$ , we will also consider the criterion involving the  $X-X$  asymmetric combination

$$\Upsilon_{m,c}^g = \frac{[\Delta(X_m^{\text{out}} + gX_c^{\text{out}})]^2 + [\Delta(P_m^{\text{out}} - gP_c^{\text{out}})]^2}{1 + g^2}. \quad (77)$$

The expressions for the inseparability parameters of the asymmetric combinations of the quadratures, Eqs. (73), are considerably more complex than that for the symmetric case and therefore we present them only graphically. Some results for the cases  $G > G_a$  and  $G_a > G$ , and for certain combinations of the parameters  $\alpha$  and  $\alpha'$ , are represented in Figs. 6(a) and (b).

Figure 6(a) shows the separability parameters  $\Delta_{a,m}^g$  and  $\Upsilon_{m,c}^g$  for the amplification case  $G > G_a$  and different numbers of the thermal photons  $n_0$ . Entanglement between the mirror and the atoms as well as between the mirror and the cavity mode is seen to occur over

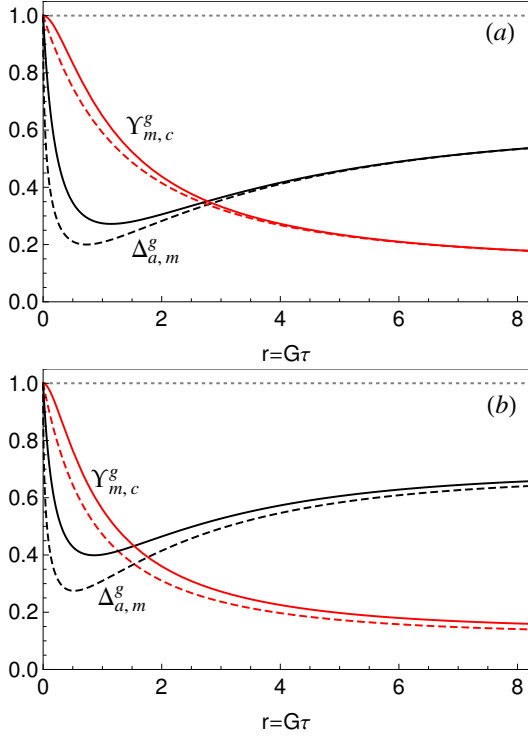


Figure 6: (Color online) The separability parameters for the asymmetric combinations of the quadrature components are shown as a function of  $r = G\tau$  for the case  $G > G_a$  with  $\alpha = 2$  (a) and for the case  $G_a > G$  with  $\alpha' = 2$  (b). Black lines represent  $\Delta_{a,m}^g$  and red lines represent  $\Upsilon_{m,c}^g$ , solid lines are for  $n_0 = 100$  and dashed lines for  $n_0 = 0$ .

the entire range of  $r$ . At small  $r$ , both  $\Delta_{a,m}^g$  and  $\Upsilon_{m,c}^g$  rapidly decrease with an increasing  $r$  but at larger  $r$  the reduction of  $\Upsilon_{m,c}^g$  is accompanied by a steady increase of  $\Delta_{a,m}^g$ . This clearly demonstrates the transfer of bipartite entanglement from the pair of modes  $(a_c, a_m)$  to the pair  $(a_m, c_a)$ . Note that in the limit of  $r \rightarrow \infty$  and  $\alpha \rightarrow \infty$ , corresponding to  $G_a \approx G$ , the parameter  $\Upsilon_{m,c}^g$  tends to zero. This indicates that in this limit the entangled state between the mirror and the atoms becomes a perfect EPR state. These results are in contrast to the symmetric case in which there is no entanglement between the mirror and the atoms, and the entanglement between the mirror and the cavity mode was restricted to small  $r$ .

In addition to the features mentioned above, one may note that the separability parameters are almost insensitive to  $n_0$  and the sensitivity becomes increasingly unimportant as  $r$  increases. This feature is also distinctly different from that seen for the symmetric criteria, in which the magnitudes of  $\Delta_{a,m}^g$ ,  $\Upsilon_{m,c}^g$  are enhanced by  $n_0$  independent of  $r$ . Moreover, the minimum value  $r_0$  required for entanglement detection via the asymmetric criteria is not limited by  $n_0$ , but in practice will depend on the accuracy achieved for selecting the gain factors, which become large, for the smaller  $r$  values in the high  $n_0$  limit.

Figure 6(b) shows the corresponding situation for the

case  $G_a > G$ . We see that similar to the case  $G > G_a$ , entanglement between the mirror and the atoms as well as between the mirror and the cavity mode is seen to occur over the entire range of  $r$ . In the limits of  $r \rightarrow \infty$  and  $\alpha' \rightarrow \infty$ , the entangled state between the mirror and the atoms becomes a perfect EPR state. We should mention that the results presented in Fig. 6(b) are essentially the same as that presented in Fig. 6(a) for the case  $G > G_a$ . We therefore conclude that in both cases the asymmetric criteria predict essentially the same features for entanglement. It then follows that the symmetric criteria cannot properly distinguish the bipartite entanglement in the system. Despite this, the criteria clearly demonstrate the role of the parametric coupling between the cavity mode and the mirror in the creation of bipartite entanglement between any other pair of the modes.

#### IV. TRIPARTITE ENTANGLEMENT

In the previous section we have considered bipartite entanglement between the modes. However, the simultaneous coupling of all three modes can result in a tripartite entanglement. In this section we discuss how such tripartite entanglement may be generated in our three-mode system. To see if a tripartite entanglement exists in the system we shall consider criteria involving variances of the sums of suitably chosen combinations of the quadrature operators of the three modes. We shall make use of the relations between the input and output fields given in Eqs. (A1)-(A4), and again we discuss the cases  $G > G_a$  and  $G_a > G$  separately.

In order to distinguish tripartite entanglement, we adopt the full inseparability criterion of three modes. Within this criterion, there is to be found two forms which involve either sums or products of the variances of linear combinations of the quadrature operators. We shall also consider a generalization of the full inseparability criterion to a criterion for genuine tripartite entanglement.

It may readily be shown using Eqs. (A1)-(A4) that the criterion for full inseparability of our three modes requires that any two of the following three inequalities are violated [32, 36, 37]

$$\begin{aligned} [\Delta(X_a + P_m)]^2 + [\Delta(P_a + X_m + g_c X_c)]^2 &\geq 2, \\ [\Delta(X_a + P_c)]^2 + [\Delta(P_a + X_c + g_m X_m)]^2 &\geq 2, \\ [\Delta(X_m + X_c)]^2 + [\Delta(P_m - P_c + g_a X_a)]^2 &\geq 2, \end{aligned} \quad (78)$$

in order for the three modes to exhibit fully inseparable tripartite entanglement. In Eq. (78),  $g_k$  ( $k = a, m, c$ ) are weight factors which with the choice to ensure minimal values of the variances. It should be noted that a violation of only one of the inequalities (78) signals the existence of some entanglement but is not sufficient for full inseparability.

Alternatively, one could setup a criterion involving products of the variances instead of the sums as the set

of the inequalities (78) can be written in a form of uncertainty principle [33]

$$\begin{aligned}\Delta_{am} &= \Delta(X_a + P_m)\Delta(P_a + X_m + g_c X_c) \geq 1, \\ \Delta_{ac} &= \Delta(X_a + P_c)\Delta(P_a + X_c + g_m X_m) \geq 1, \\ \Delta_{mc} &= \Delta(X_m + X_c)\Delta(P_m - P_c + g_a X_a) \geq 1.\end{aligned}\quad (79)$$

Each of the parameters  $\Delta_{ij}$  is evaluated with the help of the output-input relations given by Eqs. (A1)-(A4). The criterion (79) is stronger than (78), since if it holds, the criterion (78) will also hold. Similar as for the criterion (78), violation of only one of the inequalities signals the existence of some entanglement. Violation of any two of the inequalities demonstrates that the state is fully inseparable.

The criterion for full inseparability can be generalized to that for the existence of genuine tripartite entanglement [33, 34, 38] by the requirement that

$$\Delta_{\text{sum}} = \sum \Delta_{ij} < 2, \quad (80)$$

where the sum is over all the parameters  $\Delta_{ij}$ . Other witnesses of genuine tripartite entanglement have also been generalized by testing only one inequality but with fixed gains [32, 34, 37]. Here, we focus on the inequality (79) and then inequality (80) to see whether these three modes are partially inseparable, fully inseparable, or genuinely entangled.

The variation of the parameters  $\Delta_{ij}$  with  $r$  for the case  $G > G_a$  is shown in Fig. 7, where frame (a) is for symmetric, while frame (b) is for asymmetric combinations of the quadrature components. Also shown is  $\Delta_{\text{sum}}$ . We observe that in both cases there is a range of  $r$  at which two parameters of  $\Delta_{am}$ ,  $\Delta_{ac}$ , and  $\Delta_{mc}$ , are simultaneously less than 1. This means that fully inseparable tripartite entanglement can be realized in the system. Moreover, the sum  $\Delta_{\text{sum}}$  is seen to be less than 2 in some range of  $r$  indicating that genuine tripartite entanglement is realized. With the minimized variances, shown in Fig. 7(b), the fully inseparable and genuine tripartite entanglements occur over a larger range of  $r$  than in the symmetric case.

The lack of the genuine tripartite entanglement at large  $r$  can be regarded to the fact that in the case  $G > G_a$  there is a strong tendency of the system to behave as a two-mode rather than a three-mode system. We have seen in Sec. III A that for symmetric combinations of the quadrature operators, a large bipartite entanglement occurs only between the cavity and the superposition  $w$  modes, see Fig. 3. The similar situation was seen for antisymmetric combinations of the quadrature operators, illustrated in Figs. 6 and 7, where a large bipartite entanglement was seen only between the mirror and atomic modes at large  $r$ . Thus, we may conclude that tripartite entanglement is ruled out at the cases where a large bipartite entanglement is present.

Figure 8 shows the same situation as in Fig. 7 but for  $G_a > G$ . We see that in the symmetric case there is no

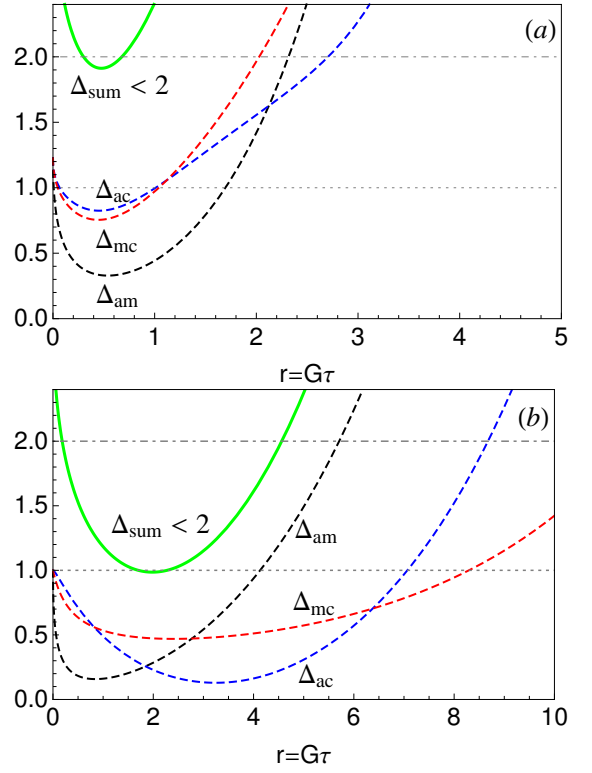


Figure 7: Variation of the parameters  $\Delta_{ij}$  and  $\Delta_{\text{sum}}$  with  $r = G\tau$  is shown for the case  $G > G_a$  with  $n_0 = 0, \alpha = 2$  for (a) symmetric combinations of the quadrature operators ( $g_a = g_m = g_c = 1$ ), (b) asymmetric combinations of the quadrature operators with optimal weight factors. The dashed line shows  $\Delta_{am}$  (black),  $\Delta_{ac}$  (blue), and  $\Delta_{mc}$  (red). The solid green line shows  $\Delta_{\text{sum}}$ .

a significant difference between the cases  $G > G_a$  and  $G_a > G$ . However, for the asymmetric case, the genuine tripartite entanglement is present over all values of  $r$ .

The explanation again follows from the observation that the presence of a tripartite entanglement is accompanied by a smaller bipartite entanglement. In Sec. III B we saw that in the case with  $G_a > G$  there is no entanglement between the cavity mode and the superposition mode  $w$ . Thus, the entangled behaves of the system do not tend to that of a two-mode system. The fluctuations is redistributed more evenly between the other three pairs of modes. This resulted in a smaller bipartite entanglement.

We may conclude that the two cases of  $G > G_a$  and  $G_a > G$  lead to quite different results not only for the bipartite but also for tripartite entanglement. It is interesting to note from Figs. 7 and 8 that the variation of the genuine tripartite entanglement with  $r$  follows the variation of  $\Delta_{a,m}$ . This suggests that the presence of an entanglement between the mirror and the cavity mode is crucial for the genuine entanglement between the modes.

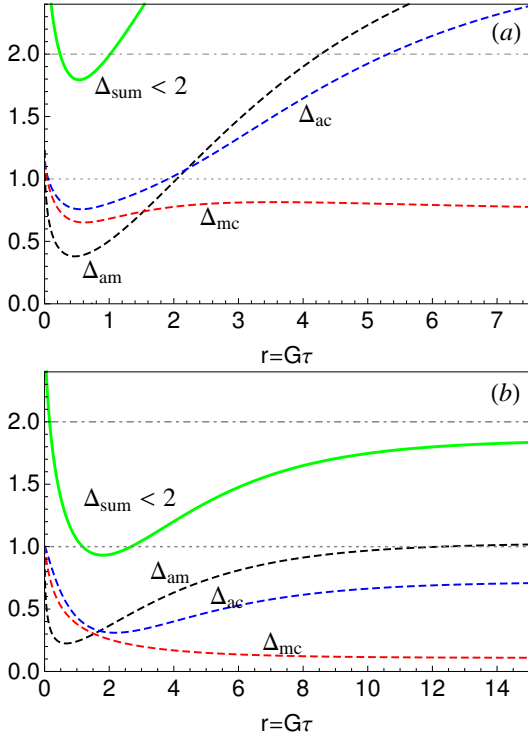


Figure 8: (Color online) Same as in Fig. 7 but for the case  $G_a > G$  with  $n_0 = 0$ ,  $\alpha' = 2$ .

## V. QUANTUM STEERING

We have seen in Sec. III that in the case with  $G > G_a$ , a bipartite entanglement created between the mirror and the cavity mode was then transferred to a pair of modes composed of the superposition mode  $w$  and the cavity mode. However, for the case with  $G_a > G$ , the entanglement was found to be transferred to a different pair of modes composed of the mirror and the atomic modes. It suggests that a kind of steering behavior exists in the system that depending on whether  $G > G_a$  or  $G_a > G$ , the entanglement can be transferred into different pairs of the modes. For this reason, we consider in this section the effect of quantum steering that provides the information how a given mode steers the other modes to be entangled. In particular, is the steering directional? Also is it one-way or two-way steering? Moreover, is the steering monogamic that if the mode  $A$  steers  $B$  then can a mode  $C$  too steers  $B$ ?

In order to develop our discussion to the problem of quantum steering, we introduce the steering parameter defined as [39–41]

$$E_{B|A} = \Delta_{inf,A} X_B \Delta_{inf,A} P_B, \quad (81)$$

where  $\Delta_{inf,A} X_B \equiv \Delta(X_B|O_A)$  and  $\Delta_{inf,A} P_B \equiv \Delta(P_B|O'_A)$  are the variances of the conditional distributions  $P(X_B|O_A)$  and  $P(P_B|O'_A)$ , in which  $O_A$ ,  $O'_A$  are arbitrary observables of the system  $A$ , usually selected to minimize the variance product [41, 42]. Quantum steer-

ing exists if

$$E_{B|A} < 1/2. \quad (82)$$

Note the inherent asymmetry of the steering parameter (81) that  $E_{B|A} < 1/2$  does not necessary mean that  $E_{A|B} < 1/2$ . We shall refer to the situation of  $E_{B|A} < 1/2$  and  $E_{A|B} > 1/2$  as the one-way steering, and for  $E_{B|A} < 1/2$  and  $E_{A|B} < 1/2$  as a two-way steering. The asymmetry reflects the asymmetric nature of the original EPR paradox, in which it is the reduced noise levels of Alice's predictions for Bob's system that are relevant in establishing the paradox [43, 44].

To see the quantum steering existing between the modes of our optomechanical system we examine the conditional probabilities of the output modes

$$\Delta_{inf}(X_i^{\text{out}}|O_j^{\text{out}}) = \Delta(X_i^{\text{out}} + g_j O_j^{\text{out}}), \quad (83)$$

where the quadrature  $O_j$  is selected either  $O_j \equiv X_j$  or  $O_j \equiv P_j$ , depending on the type of the correlations between the modes  $i$  and  $j$ . The variances are minimized with the choice of the weight factor

$$g_j = -\frac{(\langle X_i^{\text{out}}, O_j^{\text{out}} \rangle + \langle P_i^{\text{out}}, O_j^{\text{out}} \rangle)}{2(\Delta O_j^{\text{out}})^2}. \quad (84)$$

In the following part, we give illustrative figures of the behavior of the steering parameters  $E_{j|i}$  as a function of  $r$  for the two cases  $G > G_a$  and  $G_a > G$ . Comparison is made with the monogamy results and the monogamy inequalities for tripartite quantum steering recently derived by Reid [34].

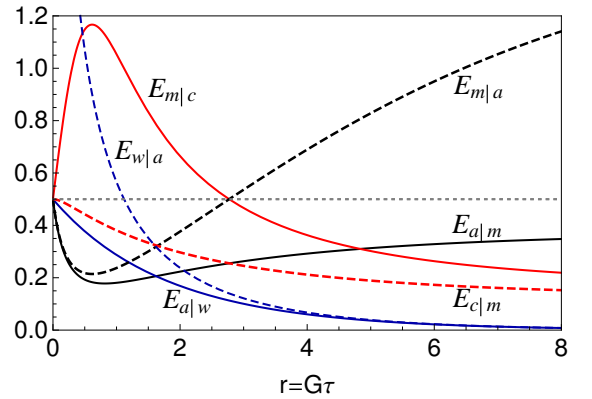


Figure 9: Variation of the steering parameters  $E_{i|j}$  with  $r$  for the case  $G > G_a$ ,  $n_0 = 0$  and  $\alpha = 2$  ( $G_a = 0.75G$ ). The solid lines show  $E_{a|m}$  (black),  $E_{m|c}$  (red), and  $E_{a|w}$  (blue). The dashed lines show  $E_{m|a}$  (black),  $E_{c|m}$  (red), and  $E_{w|a}$  (blue).

Figure 9 shows the variation of the steering parameters with  $r$  for the case  $G > G_a$ . The figure illustrates several interesting features, in particular, about steering monogamy and its directionality. By inspection of the figure, we note:

1.  $E_{a|c} > 1/2$  and  $E_{c|a} > 1/2$  over the entire range of  $r$ . Thus, neither the cavity mode steers the atomic mode nor the atomic mode steers the cavity mode. It is easy to understand owing to the beamsplitter type coupling between the modes.
2.  $E_{a|w} < 1/2$  over the entire range of  $r$  while  $E_{w|a} < 1/2$  only for  $r$  greater than a some minimum value  $r_0$ . This means that the mode  $w$  always steers the cavity mode, but the cavity mode steers  $w$  in a limited range for  $r$ . This also means that at  $r \leq r_0$ , one-way steering occurs between the modes, and it turns into a two-way steering at  $r > r_0$ . This is in agreement with the result found for quantum steering in a two-mode optomechanical system [27].
3. The cavity and the mirror modes exhibit a quite different steering behavior that  $E_{a|m} < 1/2$  and  $E_{m|a} < 1/2$  over a wide range of  $r$  but the  $E_{m|a}$  steering ceases at a large  $r$ . It is interested that the behavior of  $E_{a|m}$  and  $E_{m|a}$  is not linked to the behavior of  $E_{a|w}$  and  $E_{w|a}$  but rather to the behavior of  $E_{m|c}$  and  $E_{c|m}$ . It is clearly seen from Fig. 9 that the steering  $E_{m|c}$  emerges at the same value of  $r$  where the steering  $E_{m|a}$  ceases. This feature is consistent with the monogamy result for quantum steering that two parties, the cavity and atomic modes, cannot steer the same system, the mirror mode.
4. According to the monogamy results of Reid [34], two parties cannot steer the same system, but a given system can steer two other systems. This feature is also seen in our system. It is evident from Fig. 9 that  $E_{a|m} < 1/2$  and  $E_{c|m} < 1/2$  over the entire range of  $r$ . Thus, the dual steering is realized that the mirror steers both the cavity mode and the atomic mode. Notice the presence of an another dual steering that also  $E_{a|m} < 1/2$  and  $E_{a|w} < 1/2$  over the entire range of  $r$ .
5. The monogamy relation of preventing the passing on of steering is also seen in the system. Namely, it is seen from the figure that  $E_{m|a} < 1/2$  and  $E_{c|m} < 1/2$  but  $E_{a|c} > 1/2$ . In other words, the cavity mode steers the mirror and simultaneously the mirror steers the atomic mode, but the atomic mode does not steer the cavity mode.
6. A detailed inspection of the figure reveals that at small  $r$ , both  $E_{a|m} < 1/2$  and  $E_{a|w} < 1/2$ . Clearly, the mirror and the mode  $w$  simultaneously steer the cavity mode. This result seems to contradict the monogamy relation that two parties cannot steer the same system. However, the mirror and the superposition mode  $w$  are not separate parties. The mode  $w$  is a linear superposition of the mirror and the atomic modes. In other words, the mirror mode is a part of the mode  $w$  and as such the modes cannot be treated as separate parties.

7. It is easily verified that the monogamy inequalities  $E_{a|m}E_{a|c} \geq E_{a|w}^2$  and  $E_{a|m} + E_{a|c} \geq 2E_{a|w}$  are also satisfied. However, the inequality  $E_{a|m} \geq E_{a|w}$  is violated at small  $r$ . It is not difficult to see from Fig. 9 that for large  $r$ ,  $E_{a|m} \geq E_{a|w}$ , but for small  $r$ ,  $E_{a|m} < E_{a|w}$ . This discrepancy could be understood by noting that at small  $r$  the state of the system is not in an EPR state. The inequality is satisfied at large  $r$  where the state of the system approaches an EPR state.

Figure 10 shows the steering parameters for  $G_a > G$ . We see that the dependence of the steering parameters on  $r$  is strikingly similar to that shown in Fig. 9 for the case  $G > G_a$ . Therefore, we are not going to give a detailed discussion of the results. We just only point out that the only difference between the two cases is that in the present case there is no steering neither between the cavity mode and the mode  $w$  nor between  $w$  and the cavity mode, i.e.  $E_{a|w} > 1/2$  and  $E_{w|a} > 1/2$  for the entire range of  $r'$  and all the parameter's value.

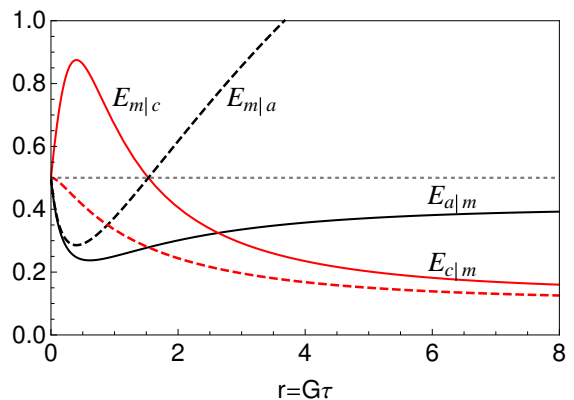


Figure 10: Variation of the steering parameters  $E_{i|j}$  with  $r$  for the case  $G_a > G$ ,  $n_0 = 0$  and  $\alpha' = 2$  ( $G_a = 4G/3$ ). The black solid line shows  $E_{a|m}$ , the black dashed line  $E_{m|a}$ , the red solid line  $E_{m|c}$ , and the red dashed line  $E_{c|m}$ .

In summary of this section, we have shown that the mirror is more capable for steering of entanglement than the cavity mode which is driven by a pulsed laser. The two way steering is found between the mirror and the atomic ensemble despite the fact that they are not directly coupled to each other. No quantum steering between the cavity mode and the ensemble which are directly coupled to each other. The reason is in the beamsplitter coupling between the modes. Thus, the results show that there must be the parametric-type coupling present in the system, at least between two modes.

## VI. CONCLUSIONS

We have examined entangled properties and quantum steering of a three-mode optomechanical system composed of an atomic ensemble located inside a single-mode

cavity with a movable mirror and driven by a short laser pulse. Using the linearization approach, we have derive analytical expressions for the output-input relations between the amplitudes of the fields. We have found a threshold effect for the dynamics of the system imposed by the ratio  $G/G_a$  of the coupling strengths of the oscillating mirror to the cavity mode and the cavity mode to the atoms. Above the threshold ( $G > G_a$ ), the system behaves as an amplifier, whereas below the threshold ( $G < G_a$ ), the system behaves as an attenuator of the input laser pulses. We have shown that bipartite entanglement can be generated in both amplification and attenuation regimes but a perfect bipartite EPR state can be generated only in the amplification regime. The results show that in the amplification regime the system tends to behave as a two-mode system composed of the cavity mode and a superposition of the mirror and atomic modes.

We have also considered the inseparability criteria for tripartite entanglement and have found that not only fully inseparable tripartite entanglement but also genuine tripartite entanglement can be realized in the system. The results show that in the amplification, the bipartite and tripartite entanglements exclude each other that a large tripartite entanglement is predicted in the range of the parameters where the bipartite entanglement is small or even absent. The results are different for the attenuation where tripartite entanglement occurs in the range of the parameters where the bipartite entanglement exists between the mirror and the cavity mode. The concept of quantum steering has also been investigated, in particular, the ability of the system for the directional one-way and two-way steering of entanglement. Moreover, the monogamy relations and monogamy inequalities for quantum steering have been analyzed. It has been found that the mirror is more capable for steering of entanglement than the cavity mode. The two way steering is found between the mirror and the atomic ensemble despite the fact that they are not directly coupled to each other. The mirror can steer both the cavity mode and the atomic mode. No quantum steering has been found between the directly coupled cavity mode and the atomic ensemble.

### Acknowledgments

This work was supported by the National Natural Science Foundation of China under Grant No. 11274025 and 11121091.

### Appendix A

In this Appendix we give the explicit expressions for the relations between the output and input quadrature

components of the fields. If we make use of the relations between the annihilation operators of the input and output fields and its Hermitian conjugate, Eq. (36) for  $G > G_a$ , and Eq. (47) for  $G_a > G$ , we then find the relations between the quadrature components of the input and output fields.

For the case  $G > G_0$ , the in-phase quadrature components satisfy the relations

$$\begin{aligned} X_a^{\text{out}} &= -e^{r_\alpha} X_a^{\text{in}} - \alpha \sqrt{e^{2r_\alpha} - 1} P_m^{\text{in}} + \beta \sqrt{e^{2r_\alpha} - 1} P_c^{\text{in}}, \\ X_m^{\text{out}} &= (\alpha^2 e^{r_\alpha} - \beta^2) X_m^{\text{in}} + \alpha \beta (e^{r_\alpha} - 1) X_c^{\text{in}} \\ &\quad + \alpha \sqrt{e^{2r_\alpha} - 1} P_a^{\text{in}}, \\ X_c^{\text{out}} &= (\alpha^2 - \beta^2 e^{r_\alpha}) X_c^{\text{in}} - \alpha \beta (e^{r_\alpha} - 1) X_m^{\text{in}} \\ &\quad - \beta \sqrt{e^{2r_\alpha} - 1} P_a^{\text{in}}, \end{aligned} \quad (\text{A1})$$

and for the out-off-phase quadratures

$$\begin{aligned} P_a^{\text{out}} &= -e^{r_\alpha} P_a^{\text{in}} - \alpha \sqrt{e^{2r_\alpha} - 1} X_m^{\text{in}} - \beta \sqrt{e^{2r_\alpha} - 1} X_c^{\text{in}}, \\ P_m^{\text{out}} &= (\alpha^2 e^{r_\alpha} - \beta^2) P_m^{\text{in}} - \alpha \beta (e^{r_\alpha} - 1) P_c^{\text{in}} \\ &\quad + \alpha \sqrt{e^{2r_\alpha} - 1} X_a^{\text{in}}, \\ P_c^{\text{out}} &= (\alpha^2 - \beta^2 e^{r_\alpha}) P_c^{\text{in}} + \alpha \beta (e^{r_\alpha} - 1) P_m^{\text{in}} \\ &\quad + \beta \sqrt{e^{2r_\alpha} - 1} X_a^{\text{in}}. \end{aligned} \quad (\text{A2})$$

Similarly, for the case  $G_a > G$ , we find

$$\begin{aligned} X_a^{\text{out}} &= -e^{-r'_\beta} X_a^{\text{in}} - \beta' \sqrt{1 - e^{-2r'_\beta}} P_m^{\text{in}} \\ &\quad + \alpha' \sqrt{1 - e^{-2r'_\beta}} P_c^{\text{in}}, \\ X_m^{\text{out}} &= (\alpha'^2 - \beta'^2 e^{-r'_\beta}) X_m^{\text{in}} + \alpha' \beta' (1 - e^{-r'_\beta}) X_c^{\text{in}} \\ &\quad + \beta' \sqrt{1 - e^{-2r'_\beta}} P_a^{\text{in}}, \\ X_c^{\text{out}} &= (\alpha'^2 e^{-r'_\beta} - \beta'^2) X_c^{\text{in}} - \alpha' \beta' (1 - e^{-r'_\beta}) X_m^{\text{in}} \\ &\quad - \alpha' \sqrt{1 - e^{-2r'_\beta}} P_a^{\text{in}}, \end{aligned} \quad (\text{A3})$$

and

$$\begin{aligned} P_a^{\text{out}} &= -e^{-r'_\beta} P_a^{\text{in}} - \beta' \sqrt{1 - e^{-2r'_\beta}} X_m^{\text{in}} \\ &\quad - \alpha' \sqrt{1 - e^{-2r'_\beta}} X_c^{\text{in}}, \\ P_m^{\text{out}} &= (\alpha'^2 - \beta'^2 e^{-r'_\beta}) P_m^{\text{in}} - \alpha' \beta' (1 - e^{-r'_\beta}) P_c^{\text{in}} \\ &\quad + \beta' \sqrt{1 - e^{-2r'_\beta}} X_a^{\text{in}}, \\ P_c^{\text{out}} &= (\alpha'^2 e^{-r'_\beta} - \beta'^2) P_c^{\text{in}} + \alpha' \beta' (1 - e^{-r'_\beta}) P_m^{\text{in}} \\ &\quad + \alpha' \sqrt{1 - e^{-2r'_\beta}} X_a^{\text{in}}. \end{aligned} \quad (\text{A4})$$



- 
- [1] C. Genes, A. Mari, D. Vitali, and P. Tombesi, *Adv. At. Mol. Opt. Phys.* **57**, 33 (2009).
- [2] M. Aspelmeyer, S. Gröblacher, K. Hammerer, and N. Kiesel, *J. Opt. Soc. Am. B* **27**, A189 (2010).
- [3] J. D. Teufel, T. Donner, M. A. Castellanos-Beltran, J. W. Harlow, and K. W. Lehnert, *Nature Nanotechnology* **4**, 820 (2009).
- [4] S. Gröblacher, K. Hammerer, M. R. Vanner, and M. Aspelmeyer, *Nature* **460**, 724 (2009).
- [5] A. Ferreira, A. Guerreiro, and V. Vedral, *Phys. Rev. Lett.* **96**, 060407 (2006).
- [6] D. Vitali, S. Gigan, A. Ferreira, H. R. Bohm, P. Tombesi, A. Guerreiro, V. Vedral, A. Zeilinger, and M. Aspelmeyer, *Phys. Rev. Lett.* **98**, 030405 (2007).
- [7] M. Paternostro, D. Vitali, S. Gigan, M. S. Kim, C. Brukner, J. Eisert, and M. Aspelmeyer, *Phys. Rev. Lett.* **99**, 250401 (2007).
- [8] D. Vitali, P. Tombesi, M. J. Woolley, A. C. Doherty, and G. J. Milburn, *Phys. Rev. A* **76**, 042336 (2007).
- [9] M. Bhattacharya, P. L. Giscard, and P. Meystre, *Phys. Rev. A* **77**, 013827 (2008).
- [10] C. Genes, A. Mari, P. Tombesi, and D. Vitali, *Phys. Rev. A* **78**, 032316 (2008).
- [11] H. Ian, Z. R. Gong, Y.-X. Liu, C. P. Sun, and F. Nori, *Phys. Rev. A* **78**, 013824 (2008).
- [12] M. Paternostro, G. De Chiara, and G. M. Palma, *Phys. Rev. Lett.* **104**, 243602 (2010).
- [13] G. De Chiara, M. Paternostro, and G. M. Palma, *Phys. Rev.* **83**, 052324 (2011).
- [14] S. Mancini, V. Giovannetti, D. Vitali, and P. Tombesi, *Phys. Rev. Lett.* **88**, 120401 (2002).
- [15] M. J. Hartmann and M. B. Plenio, *Phys. Rev. Lett.* **101**, 200503 (2008).
- [16] K. Hammerer, M. Wallquist, C. Genes, M. Ludwig, F. Marquardt, P. Treutlein, P. Zoller, J. Ye, and H. J. Kimble, *Phys. Rev. Lett.* **103**, 063005 (2009).
- [17] M. Wallquist, K. Hammerer, P. Zoller, C. Genes, M. Ludwig, F. Marquardt, P. Treutlein, J. Ye, and H. J. Kimble, *Phys. Rev. A* **81**, 023816 (2010).
- [18] S. Camerer, M. Korppi, A. Jockel, D. Hunger, T. W. Hansch, and P. Treutlein, *Phys. Rev. Lett.* **107**, 223001 (2011).
- [19] J. D. Jost, J. P. Home, J. M. Amini, D. Hanneke, R. Ozeri, C. Langer, J. J. Bollinger, D. Leibfried, and D. J. Wineland, *Nature* **459**, 683 (2009).
- [20] Sh. Barzanjeh, D. Vitali, P. Tombesi, and G. J. Milburn, *Phys. Rev. A* **84**, 042342 (2011).
- [21] L. Zhou, Y. Han, J. Jing, and W. Zhang, *Phys. Rev. A* **83**, 052117 (2011).
- [22] H. Tan, F. Bariani, G. X. Li, and P. Meystre, *Phys. Rev. A* **88**, 023817 (2013).
- [23] C. Genes, D. Vitali, and P. Tombesi, *Phys. Rev. A* **77**, 050307(R) (2008).
- [24] L. H. Sun, G. X. Li, and Z. Ficek, *Phys. Rev. A* **85**, 022327 (2012).
- [25] Y. D. Wang and A. A. Clerk, *Phys. Rev. Lett.* **110**, 253601 (2013).
- [26] S. G. Hofer, W. Wieczorek, M. Aspelmeyer, and K. Hammerer, *Phys. Rev. A* **84**, 052327 (2011).
- [27] Q. Y. He and M. D. Reid, *Phys. Rev. A* **88**, 052121 (2013).
- [28] Y. S. Bai, A. G. Yodh, and T. W. Mossberg, *Phys. Rev. Lett.* **55**, 1277 (1985).
- [29] L. M. Duan, G. Giedke, J. I. Cirac, and P. Zoller, *Phys. Rev. Lett.* **84**, 2722 (2000).
- [30] R. Simon, *Phys. Rev. Lett.* **84**, 2726 (2000).
- [31] V. Giovannetti, S. Mancini, D. Vitali, and P. Tombesi, *Phys. Rev. A* **67**, 022320 (2003).
- [32] P. van Loock and A. Furusawa, *Phys. Rev. A* **67**, 052315 (2003).
- [33] L. K. Shalm, D. R. Hamel, Z. Yan, C. Simon, K. J. Resch, and T. Jennewein, *Nature Physics* **9**, 19 (2012).
- [34] M. D. Reid, arXiv:1310.2690.
- [35] M. D. Reid, arXiv:1310.2729.
- [36] W. Dur, J. I. Cirac, and R. Tarrach, *Phys. Rev. Lett.* **83**, 3562 (1999).
- [37] A. S. Bradley, M. K. Olsen, O. Pfister, and R. C. Pooser, *Phys. Rev. A* **72**, 053805 (2005); C. Pennarun, A. S. Bradley, and M. K. Olsen, *Phys. Rev. A* **76**, 063812 (2007).
- [38] M. Bourennane et al., *Phys. Rev. Lett.* **92**, 087902 (2004).
- [39] M. D. Reid, *Phys. Rev. A* **40**, 913 (1989).
- [40] H. M. Wiseman, S. J. Jones, and A. C. Doherty, *Phys. Rev. Lett.* **98**, 140402 (2007).
- [41] E. G. Cavalcanti, S. J. Jones, H. M. Wiseman, and M. D. Reid, *Phys. Rev. A* **80**, 032112 (2009).
- [42] M. D. Reid et al., *Rev. Mod. Phys.* **81**, 1727 (2009) and references therein.
- [43] A. Einstein, B. Podolsky, and N. Rosen, *Phys. Rev.* **47**, 777 (1935).
- [44] V. Hndchen et al., *Nature Photonics* **6**, 598 (2012); K. Wagner et al., arXiv:1203.1980 [quant-ph].